

# **ATOM TRANSFER RADICAL POLYMERIZATION IN MICROEMULSION**

by

Di Jia

A thesis submitted to the Department of Chemical Engineering

In conformity with the requirements for  
the degree of Master of Science (Engineering)

Queen's University

Kingston, Ontario, Canada

(January, 2008)

Copyright © Di Jia, 2008

## Abstract

Living/controlled radical polymerization (L/CRP) techniques in aqueous based systems were studied. The main focus of this research was adapting an ATRP (atom transfer radical polymerization) to a microemulsion polymerization in order to form nano-size particles with low concentration of surfactant.

In conventional microemulsion polymerization, the cationic surfactant cetyltrimethylammonium bromide (CTAB) was successfully employed with a low weight ratio of surfactant/monomer of 1:10 to produce polymer particles with mean diameters less than 40 nm. Poor control resulted when this microemulsion polymerization was used with reverse ATRP, but using acetone as a phase transfer agent improved the results.

The AGET (activators generated by electron transfer) initiation technique was also employed in microemulsion ATRP. In this “two-step” procedure, a reducing agent, ascorbic acid, was used to reduce the higher oxidation state catalyst in situ during the first stage to initiate a microemulsion polymerization. Monomer was then continuously fed to the microemulsion ATRP to form the final polymer latex. In an effort to improve this microemulsion polymerization, factors such as the catalyst concentration, temperature, and surfactant concentration were studied. Two monomers, butyl acrylate (BA) and butyl methacrylate (BMA) were investigated. When BA was used, linear first-order kinetic plots and relatively narrow molecular weight distribution ( $M_w/M_n \sim 1.5$ ) were observed. The final latex had a particle size  $\sim 20$  nm. When BMA was employed, very fast reaction rates were obtained, leading to poorly controlled polymerizations with quite high polydispersity ( $M_w/M_n \sim 2$ ). The two-step AGET ATRP procedure in microemulsion provides options for synthesizing polymer nano-particles with low concentration surfactant in aqueous dispersed media.

## **Acknowledgements**

I would like to thank my supervisor Dr. Michael F. Cunningham for the great opportunity to work in his lab over the last two years. Thanks for his enthusiasm, support, advice and supervision.

Many thanks also go to all my lab mates over the years. With them, life was enjoyable in the lab. Thanks for their help and advice, I learned a lot from them.

Thanks to my family. Without their support, the work cannot be done in time.

## Table of Contents

Abstract.....	ii
Acknowledgements.....	iii
Table of Contents.....	iv
List of Figures.....	vi
List of Tables.....	viii
Nomenclature.....	ix
Chapter 1 Introduction.....	1
Chapter 2 Literature Review.....	3
2.1 Living/Controlled Radical Polymerization (L/CRP).....	3
2.2 Atom Transfer Radical Polymerization (ATRP).....	4
2.2.1 Overview.....	4
2.2.2 Recent Development in ATRP.....	6
2.2.3 Conclusion.....	9
2.3 Microemulsion Polymerization.....	10
2.3.1 Introduction.....	10
2.3.2 Techniques for making nanoparticles.....	10
2.3.3 Properties and uses of nanoparticles.....	13
2.3.4 Conclusion.....	13
2.4 Scope of research in this thesis.....	14
Chapter 3 Experimental.....	15
3.1 Materials.....	15
3.2 Analysis.....	17
3.2.1 Conversion.....	17
3.2.2 Gel Permeation Chromatography (GPC).....	17
3.2.3 Capillary Hydrodynamic Fractionation (CHDF).....	18
3.2.4 Dynamic Light Scattering (DLS).....	18
Chapter 4 Atom Transfer Radical Polymerization (ATRP).....	19
4.1 Conventional microemulsion polymerization.....	19
4.1.1 Experimental procedure.....	19
4.1.2 Results and discussion.....	20
4.2 ATRP in microemulsion polymerization.....	20
4.2.1 Experimental procedure.....	21

4.2.2 Results and discussion .....	21
4.3 Seeded microemulsion polymerization.....	24
4.3.1 Experimental Procedure.....	24
4.3.2 Results and discussion .....	26
4.4 Conclusion .....	29
Chapter 5 Generating Nano-sized PolyButyl Acrylate using AGET ATRP.....	30
5.1 Introduction.....	30
5.2 Experimental.....	31
5.3 Results and Discussion .....	32
5.3.1 Effect of the catalyst concentration.....	32
5.3.2 Effect of the surfactant concentration .....	38
5.3.3 Effect of surfactants (CTAB vs. Brij98) .....	42
5.3.4 Effect of ligands (BPMODA vs. EHA <sub>6</sub> -TREN) .....	47
5.3.5 Effect of monomer addition and temperature .....	53
5.4 Conclusion .....	59
Chapter 6 AGET ATRP of Butyl Methacrylate.....	60
6.1 Introduction.....	60
6.2 Experimental.....	61
6.3 Results and Discussion .....	62
6.4 Conclusion .....	73
Chapter 7 Conclusions .....	75
Chapter 8 Recommendations for Future Work.....	76
Appendix.....	82

## List of Figures

Figure 2- 1 Mechanism of metal complex-mediated ATRP .....	4
Figure 2- 2 Scheme of the AGET ATRP method .....	7
Figure 3- 1 Structures of EHA <sub>6</sub> -TREN and BPMODA .....	16
Figure 4- 1 (a) time course curve of conversion and (b) Mn vs. conversion in BMA ATRP microemulsion.....	23
Figure 4- 2 Conversion as a function of time of BMA in seeded ATRP microemulsion polymerization .....	27
Figure 4- 3 Evolution of molecular weight (M <sub>n</sub> ) of BMA in seeded ATRP microemulsion polymerization by using acetone as transfer agent. ....	28
Figure 5- 1 Effect of catalyst concentration on BA polymerization (a) First-order kinetic plots (b) Evolution of Molecular weight versus conversion. ....	33
Figure 5- 2 Effect of catalyst concentration on GPC traces for AGET ATRP of BA in a microemulsion [CuBr <sub>2</sub> ]: [EBiB] = r = 0.74 (a), 0.9 (b) and 1.3 (c) .....	36
Figure 5- 3 Effect of surfactant concentration on BA polymerization (a) first-order kinetic plots and (b) evolution of Mn .....	40
Figure 5- 4 GPC traces on the effect of surfactant concentration on BA AGET ATRP [CTAB]/ [BA] (wt %) equals to (a) 37.2 (b) 27.6 and (c) 35.8 .....	42
Figure 5- 5 Comparison of Brij98 and CTAB on BA polymerization (a) conversion evolution and (b) molecular weight dependence [CuBr <sub>2</sub> ]/ [EBiB] = 0.5, .....	44
Figure 5- 6 Comparison of Brij98 and CTAB on GPC traces (a) [CTAB]: [BA] = 35.8 wt %, (b) [Brij98]: [BA] = 36.6 wt %, .....	46
Figure 5- 7 Comparison of BPMODA and EHA <sub>6</sub> -TREN (a) first-order plots and (b) evolution of Mn versus conversion.....	49
Figure 5- 8 GPC traces of BA polymerization using CuBr <sub>2</sub> /EHA <sub>6</sub> -TREN as the catalyst ....	50
Figure 5- 9 Comparison of BPMODA and EHA <sub>6</sub> -TREN (a) first-order plots and (b) evolution of Mn versus conversion.....	51
Figure 5- 10 GPC traces of BA polymerization using CuBr <sub>2</sub> /EHA <sub>6</sub> -TREN as the catalyst...	52
Figure 5- 11 Comparison of differential method and batch method (a) first-order kinetic plots and (b) molecular weight dependence.....	54
Figure 5- 12 Comparison of batch method (a) and differential method (b) on GPC traces...	55
Figure 5- 13 The effect of temperature on BA polymerization (a) First-order kinetic plots and (b) evolution of Mn and Mw/Mn versus conversion.....	57

Figure 5- 14 GPC traces of the effect of temperature on BA polymerization (a) 90°C and (b) 80°C .....	58
Figure 6- 1 The effect of Temperature on BMA polymerization (a) first-order plots and (b) Mn vs. Conversion of BMA.....	64
Figure 6- 2 GPC traces of BMA polymerization at different temperature (a) 70°C, (b) 50°C, and (c) 35°C .....	66
Figure 6- 3 The effect of ascorbic acid concentration on BMA polymerization (a) first-order plots and (b) molecular weight and Mw/Mn versus conversion .....	68
Figure 6- 4 The effect of surfactants on BMA polymerization (a) Conversion evolution and (b) molecular weight dependence .....	70
Figure 6- 5 The effect of degree of polymerization at the first stage on BMA polymerization (a) Conversion evolution and (b) molecular weight dependence.....	72
Figure 6- 6 GPC traces at various DPs in BMA polymerization .....	73
Figure A- 1 Evolution of conversion in reproducibility of BA in AGET ATRP microemulsion.....	83
Figure A- 2 <sup>1</sup> H NMR spectra of ligand BPMODA .....	85

## List of Tables

Table 3- 1 List of materials used in this project.....	15
Table 4- 1 Experimental conditions and results of BMA ATRP in microemulsion .....	22
Table 4- 2 Experimental conditions and results of BMA in seeded ATRP microemulsion polymerization .....	26
Table 5- 1 The effect of catalyst concentration on particle size .....	37
Table 5- 2 Experimental conditions and results for AGET ATRP of BA microemulsion polymerization on effect of surfactant concentration.....	39
Table 5- 3 The effect of Brij98 and CTAB on BA polymerization .....	43
Table 5- 4 The effect of BPMODA vs. EHA <sub>6</sub> -TREN on BA polymerization .....	47
Table 6- 1 Effect of Temperature on BMA polymerization .....	63
Table 6- 2 The effect of Brij98 on BMA polymerization .....	69

## Nomenclature

ATRP	Atom transfer radical polymerization
L/CRP	Living/controlled radical polymerization
CTAB	cetyltrimethylammonium bromide
AGET	activators generated by electron transfer
BA	butyl acrylate
BMA	butyl methacrylate
SFRP	Stable free radical polymerization
RAFT	Reverse addition fragmentation chain transfer polymerization
TEMPO	2, 2, 6, 6-tetramethyl-1-piperidynyl-N-oxy
SR&NI	simultaneous reverse and normal initiation
MMA	methyl methacrylate
BPMODA	Bis(2-pyridylmethyl) octadecylamine
SDS	sodium dodecyl sulfate
Brij98	Polyoxyethylene(20) oleyl ether
VA-044	2,2'-azobis[2-(2-imidazolin-2-yl)propane] dihydrochloride
EBiB	Ethyl 2-Bromoisobutyrate
THF	Tetrahydrofuran
EHA <sub>6</sub> -TREN	Tris[2-di(2-ethylhexylacrylate)aminoethyl]amine

# Chapter 1

## Introduction

Recently, nano-sized polymer particles have received increasing research interest since they possess many unique and special properties. For large scale industrial applications, it is very important to develop a robust method to produce nano-sized polymers with controlled molecular weight and narrow polydispersity. Ideally, the polymers should be produced in an aqueous system because of environmental concerns.

Microemulsion polymerization can be used to make nanoparticles with the particle size smaller than 20 nm for many polymers <sup>(1)</sup>. However, a large amount of surfactant usually has to be applied in this system, resulting in a complex post-treatment process and high costs. A differential microemulsion polymerization method has been used to reduce the amount of surfactant <sup>(2)</sup>, and less than 20 nm PMMA particles were obtained with a low surfactant/monomer ratio (1:18, w/w). However these results are for a traditional (non-living) polymerization, and therefore the molecular weight and molecular weight distribution were not controlled.

Living/controlled radical polymerizations (L/CRP) were developed in the last decade to produce polymers with ideal molecular weight and narrow polydispersity. Atom transfer radical polymerization (ATRP) is one of the L/CRP processes attracting commercial interest because it is robust, easy to setup and the initiators and catalysts are commercially available. However, only one study reported the synthesis of small sized nano-particles using ATRP. In a continuous “two-step” ab initio emulsion system, activators generated by electron transfer (AGET) ATRP was applied at the first step to form a microemulsion ATRP and then the remaining monomer was added into the system to form an ab initio emulsion <sup>(3)</sup>. Controlled polymers were synthesized, but the particle size was about 120 nm.

In this research, the feasibility of producing nano-sized polymer particles using ATRP in an aqueous based system with low surfactant concentration was studied. The factors affecting polymerization, particle size, and molecular weight were investigated to provide initial information for eventual application to large scale industrial applications.

L/CRP techniques are reviewed in Chapter 2. The development of ATRP is reviewed, as well as a two-step AGET ATRP procedure to produce nanoparticles, and general microemulsion polymerization. Chapter 2 also reviews a method called differential microemulsion which can form particles with diameters less than 20 nm using low amounts of surfactant. In Chapter 4, this differential microemulsion polymerization was used to synthesize polymer nanoparticles with cationic surfactant in conventional polymerization, ATRP and seeded polymerization. Small particles were obtained using a low weight ratio of surfactant/monomer, but a controlled system was not obtained. In order to produce polymer nanoparticles with predetermined molecular weight, experiments were conducted using a two-step AGET ATRP method, employing either BA or BMA as monomer. The results and discussion of these studies are reported in Chapters 5 and 6. The techniques developed in this thesis demonstrate the feasibility of producing polymer nanoparticles with controlled molecular weight distribution by using low concentrations of surfactant.

## Chapter 2

### Literature Review

Since the production of nano sized polymers with the controlled molecular weight and narrow polydispersity is a relatively new research area, a well developed method is not available in the present. However, the knowledge of producing nano sized polymer particles by microemulsion polymerization and controlling the molecular weight and polydispersity by living/controlled radical polymerization (L/CRP) is well known. In this chapter, the development of ATRP and microemulsion polymerization was reviewed and the potential of combining these two techniques to generate the controlled nano particles were illustrated.

#### 2.1 Living/Controlled Radical Polymerization (L/CRP)

Living/controlled polymerization is a synthetic method to prepare well defined polymers that are with predetermined molecular weight, narrow polydispersities, chain topologies and controlled end-group functionalities. L/CRP has the potential to become commercially viable because it provides the end-group control and the ability to synthesize polymers with complex architectures, such as block polymers, star polymers, etc. Three L/CRP approaches are presently studied extensively: stable free radical polymerization (SFRP), atom transfer radical polymerization (ATRP) and reverse addition fragmentation chain transfer polymerization (RAFT).

SFRP is using a stable radical to couple with the active radical and reversibly form a dormant species. Georges reported a controlled polymerization of styrene in the presence of benzoyl peroxide and the mediating stable free radical TEMPO (2, 2, 6, 6-tetramethyl-1-piperidynyl-N-oxy) in SFRP <sup>(4)</sup>. This reaction was conducted at 120°C and the polydispersity was below 1.3. This was the first example of a successful CRP utilizing a nitroxide-based system. SFRP was also successfully applied in seeded emulsion and miniemulsion polymerizations <sup>(5,6)</sup>. Reversible addition-fragmentation chain transfer (RAFT) is another successful L/CRP process in terms of the



The equilibrium between the two processes determines the concentration of radicals and subsequently the rates of polymerization and termination as well as polydispersities, as shown in eq. 1 and 2<sup>(8)</sup>.

The rate of polymerization is given by:

$$R_p = k_p [M] K_{\text{ATRP}} [RX] ([M_t^n / L] / [M_t^{n+1} X / L]) \quad (1)$$

Where  $R_p$  is the polymerization rate;  $k_p$  is the propagation rate constant;  $[M]$  and  $[RX]$  are the concentration of the monomer and the initiator, respectively;  $K_{\text{ATRP}}$  is the ATRP equilibrium constant; and  $[M_t^n / L] / [M_t^{n+1} X / L]$  is the molar ratio of activator to deactivator.

According to eq. 1, the polymerization rate increases with initiator concentration and also depends on the ratio of activator to deactivator concentration.

The polydispersity is given by:

$$PDI = \frac{M_w}{M_n} = 1 + \left( \frac{[RX]_0 k_p}{k_{\text{deact}} [M_t^{n+1} X / L]} \right) \left( \frac{2}{p} - 1 \right) \quad (2)$$

Where  $p$  is the conversion;  $[RX]_0$  and  $[M_t^{n+1} X / L]$  are the concentration of the initiator and the deactivator, respectively;  $k_{\text{deact}}$  is the deactivation rate constant<sup>(9)</sup>.

According to eq. 2, to synthesize polymers with low polydispersities a sufficient concentration of deactivator is required. Polydispersities become smaller with the increase of monomer conversion and deactivator concentration, and the decrease of  $k_p/k_{\text{deact}}$  ratio.

The degree of control in ATRP is strongly affected by  $K_{\text{ATRP}}$  ( $K_{\text{ATRP}} = k_{\text{act}} / k_{\text{deact}}$ ) and the activation and deactivation rates. The  $K_{\text{ATRP}}$  value can be determined experimentally. In a simple method, an alkyl halide was reacted with a transition metal activator and the increase of deactivator concentration accumulated as a persistent radical was monitored with time. The  $K_{\text{ATRP}}$  was then determined using modified Fischer's equations<sup>(8)</sup>. In a recent study, the activation rate constants were measured under a wide variety of nitrogen-based ligands. In general, the activity of the Cu-ligand complexes increased in the following order: acryl amine < acryl imine < alkyl

imine<alkyl amine~pyridine<sup>(10)</sup>. Deactivation rate constants were much less studied, owing to the lack of efficient techniques for measuring the relatively fast process ( $\sim 10^7 \text{M}^{-1} \text{s}^{-1}$ ). However,  $K_{\text{ATRP}}$  can be directly measured and  $k_{\text{deact}}$  can be determined by knowing the value of  $k_{\text{act}}$ <sup>(11)</sup>. Determination of  $k_{\text{deact}}$  is important, as it plays a critical role in the degree of control over molecular weight distribution in a controlled radical polymerization.

### 2.2.2 Recent Development in ATRP

Different ATRP procedures have been developed over time including the normal, reverse, SR&NI, AGET, ARGET and ICAR ATRP with the difference primarily in the initiation step.

#### Normal/Reverse/SR&NI ATRP

In a normal ATRP, the initiating radicals are generated from an alkyl halide in the presence of a transition metal in its lower oxidation state (e.g.,  $\text{CuBr}(\text{dNbpy})_2$ ). However, oxygen dissolving in the aqueous media will readily oxidize the transition metal in the catalyst complex, resulting in loss of the ATRP activator and reduce of the reaction rate<sup>(12)</sup>.

Reverse ATRP is a convenient method for reducing the oxidation problems<sup>(13)</sup>. In a reverse ATRP, transition metal complexes in the higher oxidation state (e.g.  $\text{Cu(II)}$  complex) are added to the reaction. Radicals are generated by decomposition of conventional free radical initiator. The components of the initial system are less sensitive to air, so this technique would be more compatible with commercial processes<sup>(14)</sup>. Cunningham's group reported a successful reverse ATRP of butyl methacrylate in miniemulsion polymerization. Cationic surfactant CTAB was employed in the system with the concentration as low as 1 wt % with respect to monomer<sup>(15)</sup>. They reported that high molecular weight polymers could be synthesized by reverse ATRP as well<sup>(16)</sup>. A redox initiation system (ascorbic acid/hydrogen peroxide) and a  $\text{CuBr}_2/\text{EHA}_6\text{-TREN}$  catalyst was used in the miniemulsion system and a controlled polymerization was successfully obtained with a high molecular weight ( $M_n \sim 10^6 \text{ g/mol}$ ) and a narrow polydispersity ( $\text{PDI} \sim 1.25$ ).

In contrast to reverse ATRP, a technique named simultaneous reverse and normal initiation (SR&NI) utilizes a dual initiation system comprising of standard free radical initiators and the higher oxidation state metal complex as well as initiators with a transferable atom or group (e.g. alkyl halide) <sup>(17)</sup>. In this process, an ATRP initiator, an alkyl halide or a halogen-terminated macroinitiator, is added to the reaction together with a conventional radical initiator. The radicals generated by the free radical initiator are deactivated by a Cu(II) X/L complex forming Cu(I) X/L. The Cu(I) X/L can then activate the alkyl halide initiator and concurrently mediate normal ATRP. However, the use of a conventional radical initiator, introduced new free radicals leading to the production of homopolymer chains. Therefore, pure block copolymers are nearly impossible to obtain by SR&NI ATRP.

#### **Activator generated by electron transfer (AGET) ATRP**

A novel procedure named activator generated by electron transfer (AGET) ATRP was developed recently (Figure 2-2) <sup>(18)</sup>. In AGET ATRP, a reducing agent is employed to generate the activator. The reducing agent reacts with the higher oxidation state transition metal complex but is unable to initiate new chains <sup>(19)</sup>. Therefore, pure linear block copolymers and star block copolymers are able to be synthesized without the presence of any homopolymers. Min reported the first miniemulsion AGET ATRP <sup>(20)</sup>. This system used alkyl halides as initiators and higher oxidation transition metal complexes (e.g. Cu(II) Br<sub>2</sub>/ligand) as catalysts.

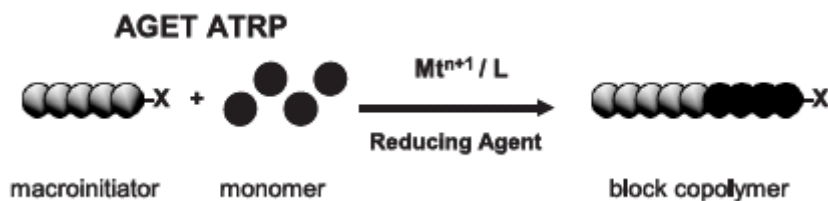


**Figure 2- 2 Scheme of the AGET ATRP method**

The AGET ATRP can be carried out in the presence of a limited amount of air in miniemulsion and in bulk polymerization <sup>(21)</sup>. Ascorbic acid and tin (II) 2-ethyl-hexanoate were used as the reducing agents in miniemulsion and bulk, respectively. An excess of reducing agent was used to consume the oxygen present in the system. The polymerization of butyl acrylate reached over 60% after 6 h and low polydispersity ( $M_w/M_n = 1.23$ ) was achieved.

AGET ATRP has significant advantages because all of these reagents are stable in the presence of air and no homopolymers are produced during block copolymerization. ATRP was successfully conducted in emulsion, miniemulsion, and suspension system. Recently, microemulsion ATRP was investigated <sup>(22)</sup>. Normal ATRP, reverse ATRP and AGET ATRP procedures were all examined in this work. Methyl methacrylate (MMA) was used as monomer, Brij98 as surfactant and Bis(2-pyridylmethyl) octadecylamine (BPMODA) as ligand. All three procedures used a higher weight ratio of surfactant to monomer ( $[\text{surfactant}]/[\text{monomer}] \sim 2.5$ ). The normal ATRP yielded bimodal peaks in the GPC trace indicating the loss of control in the polymerization. In reverse ATRP a large particle size ( $D_n = 72$  nm) was obtained, the molecular weight of polymers was higher than theoretical values, and a broad polydispersity was observed. AGET ATRP was indicated as the best choice for microemulsion. A controlled polymerization was attained with lower polydispersity ( $PDI = 1.33$ ) and small particle sizes ( $D_n \sim 38$  nm).

A continuous “two-step” procedure was developed to an ab initio emulsion system, in which a microemulsion ATRP was formed initially and then the remaining monomer was added into the system to form an ab initio emulsion <sup>(3)</sup>. The AGET technique was employed in the first stage of this ab initio ATRP to form a stable microemulsion avoiding the need of high-shear forces. The surfactant and catalyst concentration was efficiently decreased. A controlled ab initio emulsion ATRP was obtained, as evidenced by a linear first-order kinetic plot and narrow molecular weight distribution ( $M_w/M_n = 1.2-1.4$ ). The stable final latex had a particle size  $\sim 120 \pm 10$  nm.

## **ARGET/ICAR**

Because of the relatively high catalyst concentration required in ATRP, much research has been devoted to removing catalyst after polymerization. A new technique known as initiators for continuous activator regeneration (ICAR) in ATRP can be used to both scavenge oxidants and decrease the amount of catalyst needed to ppm levels leading to many industrial applications <sup>(23)</sup>.

ARGET ATRP is the most recent industrially relevant development for the production of block copolymers. In this procedure, the ATRP activator, Cu(I) species, was constantly regenerated by the reducing agents from the Cu(II) species formed during termination process. The relative concentration of catalyst to initiator could be significantly decreased to a few ppm when the reducing agent is present in excess relative to the catalyst. Well-controlled ARGET ATRP of methyl acrylate, n-butyl acrylate, methyl methacrylate, and styrene was reported by using ascorbic acid as a reducing agent <sup>(24)</sup>.

### **2.2.3 Conclusion**

The ATRP technique has numerous advantages: many transition metal complexes can be chosen as the catalysts, such as Cu, Fe and Ru, etc.; many initiators are commercially available which include various alkyl halide as well as any compound with weak halogen-hetero atom bond; a large range of monomers can be polymerized ranging from styrene, (meth)acrylates, acrylonitrile to methacrylic acid; end-functionalization is very simple; and a large range of temperatures can be employed. The limitations of ATRP include the use of relatively high amount of transition metal complex that must be removed from the final polymers <sup>(19)</sup>. However, in ARGET and ICAR initiation systems, the required catalyst levels were reduced to a few ppm levels. This is obviously beneficial to the environment. AGET ATRP has been successfully applied to an emulsion polymerization using a continuous “two-step” procedure, in which low surfactant amount was used and a controlled emulsion ATRP was obtained.

## **2.3 Microemulsion Polymerization**

### **2.3.1 Introduction**

Microemulsion polymerization has been studied since the early 1980's. A microemulsion is defined as a thermodynamically stable and optically transparent dispersion composed by water, oil and surfactant. In conventional microemulsion polymerization, a large amount of surfactant is used to form microemulsion monomer droplets and stabilize latex particles during the course of polymerization and storage. However, the use of a high surfactant concentration is unfavorable in industrial applications, due to the high surfactant cost and the post-treatment process required to remove the surfactant. Therefore, microemulsion in the low surfactant concentration is a very interesting research topic.

The mechanisms of microemulsion and miniemulsion polymerizations are significantly different. In microemulsion, large amounts of surfactant are present in the form of micelles. Micellar nucleation is the primary process of nucleation and growth. Miniemulsion polymerization involves the use of an effective surfactant/costabilizer system to produce very small (0.01-0.5 $\mu$ m) monomer droplets <sup>(52)</sup>. Particle nucleation is primarily in those monomer droplets. Microemulsions are made thermodynamically stable by using large amounts of surfactant to stabilize particles. In miniemulsion, high shear is employed to form small monomer droplets and latex stability is lower than microemulsion.

### **2.3.2 Techniques for making nanoparticles**

Generally, there are two ways to make polymer nanoparticles: polymer processing technique and polymerization. The processing technique uses the existing polymers to make nanoparticles. It is a physical technique, and no chemical reaction is involved in the process. The problem of the polymer processing methods is that special equipment is required and the final polymer must be protected from the polymer coalescence. In polymerization techniques, polymer nanoparticles are

synthesized directly from the polymerization of monomers. Miniemulsion polymerization is one of the techniques to make particles in the range of 50-500 nm. In this process, high shear equipment is employed to make the smaller monomer droplets. Subsequently, initiator is added and polymerization starts to produce fine polymer particles. In order to synthesize nanoparticles, microemulsion polymerization was developed. The microemulsion is thermodynamically stable and 10 to 50 nm particle sizes can be achieved. Traditionally, a high surfactant concentration (7-15 wt. % in the solution) is required in microemulsion polymerization processes to form stable polymer latexes and the polymer content is less than 10 wt%<sup>(25)</sup>. High surfactant levels and low polymer contents limit the application of microemulsion latexes in industry.

In order to overcome this problem, various semi-continuous microemulsion polymerizations involving drop-wise addition of monomer have been developed. In 1997, Rabelero et al.<sup>(26)</sup> first reported the production of a high solid-content (40 wt. %) polystyrene latex by semi-continuous addition of styrene to a low solid-content (6 wt %) polystyrene latex. The initial microemulsion consisted of 6 wt. % styrene, 14.1 wt. % DTAB, and 79.9 wt. % water. It is estimated that the weight ratio of polystyrene to DTAB was about 3 to 1. Gan et al.<sup>(27)</sup> used a cationic surfactant to polymerize styrene in a three-component system similar to the Winsor I system. A high styrene/DTAB weight ratio (15:1) was used and the particle size was in the range of 46-95 nm, with the polystyrene content of 15 wt. %. Dan et al.<sup>(28)</sup> studied the microemulsion polymerization of MMA by a semi-continuous feeding using sodium dodecyl sulfate (SDS) as the emulsifier. Stable and transparent PMMA microlatexes was obtained with the polymer content of ~30-40%, and the small particle size ( $D_p < 40$  nm) using the low weight ratio of emulsifier to monomer (less than or equal to 0.05).

Ming et al.<sup>(29)</sup> reported the polymerization of MMA by a modified microemulsion polymerization, i.e., continuous and slow addition of monomer (MMA) to the polymerizing MMA microemulsion with mild stirring. Their modified method produced 6-24 wt. % PMMA in microlatexes with 33-46 nm in size using about 1 wt. % DTAB (in solution). In their another study<sup>(30)</sup>, 1.0-1.5 wt. %

sodium dodecyl sulfate (SDS), 0.5-2.0 wt. % of styrene, 0.2 wt.% pentanol was used and in the original microemulsion containing a redox initiator. The additional monomer was then added dropwise into the polymerizing microemulsion at 40°C. High polymer contents of microlatexes (up to 30wt. %) with small sizes ( $D_n=10-20$  nm) were obtained.

Hermanson and Kaler <sup>(31)</sup> studied the kinetics and mechanism of the semi-continuous microemulsion polymerization of hexyl methacrylate using DTAB and DDAB as surfactants. The results showed that radicals initiated prior to monomer addition did not polymerize the added monomer probably due to either diffusion limitation within preexisting particles or to the termination of preexisting radicals by chain transfer to surfactant.

He et al. <sup>(1;2)</sup> reported the synthesis of poly (methyl methacrylate) PMMA and polystyrene nanoparticles using a method, termed differential microemulsion polymerization, which is based on a similar principle as semi-continuous microemulsion polymerization. A small amount of monomer was added into the reactor first to start the reaction, and then the remaining monomer was added in a differential manner (continuous addition in very small drops). The PMMA particles obtained were less than 20 nm with a low surfactant/monomer weight ratio of 1:18. However, the process is not capable of making polystyrene nanoparticles with a size of less than 20 nm at a low surfactant amount, probably because styrene is more oil-soluble than MMA so that it has a stronger tendency to form oil droplets.

With the technique described above, nano sized latexes containing high polymer content have been obtained by various semi-continuous microemulsion polymerizations in the low surfactant concentrations. Differential microemulsion polymerization can be used to synthesize particles less than 20nm in diameter with low weight ratio of surfactant/monomer. Though small polymer particles were produced, the polymers usually displayed high molecular weight and broad molecular weight distribution in the traditional microemulsion.

### 2.3.3 Properties and uses of nanoparticles

Polymer nanoparticles obtained by microemulsion polymerization may have some ordered chains in the particle and  $T_g$  is usually higher than the polymer particles obtained from the emulsion polymerization method. Qian et al. <sup>(32)</sup> studied single-chain polystyrene and found a dramatic difference between polystyrene made by microemulsion polymerization and commercial polystyrene polymerization. Produced by microemulsion, one exothermic peak appeared on the DSC curve when the polystyrene sample is first heated to 150°C, while commercial polystyrene has no such a peak. The  $T_g$  of polystyrene (104°C) obtained by microemulsion polymerization was just slightly higher than that of commercial polystyrene (94°C). Pilcher and Ford <sup>(33)</sup> reported structure and properties of PMMA nanoparticles. They found that the  $T_g$  of PMMA obtained by microemulsion polymerization was 125-126°C, which is much higher than 105-107°C for commercial samples and 115-117°C for materials produced by bulk polymerization.

Potential applications for polymer nanoparticles include drug delivery, micro encapsulation, and oil recovery. Polymer nanoparticles smaller than 50 nm can form a very compact monolayer and this property has been used in the coating industry <sup>(34)</sup>. In the preparation of a high performance coating, the application of nanoparticles of polyacrylic resin greatly increased the open time of the coating and improved its properties.

### 2.3.4 Conclusion

Polymer nanoparticles can be prepared either by a polymer processing method or by a polymerization method. Polymerization methods are suitable to make smaller particles. Since conventional microemulsion polymerization requires a high surfactant concentration, the semi-continuous polymerization method has been developed to prepare polymer latexes with high solid content and small particle size ranging from 20 to 80 nm. The differential microemulsion polymerization was able to produce less than 20 nm polymer particles and was very attractive.

## **2.4 Scope of research in this thesis**

ATRP is a powerful tool to produce polymers with controlled molecular weight and narrow polydispersity. The application of ATRP in microemulsion was reported but limited by the use of high surfactant concentration. The recent advance in the microemulsion might provide a solution for this problem. In this research, a “two-step” AGET ATRP was applied to microemulsion polymerization by the “differential method” to produce controlled nanoparticles with the low surfactant concentration. In the first step, all ATRP initiators, catalysts and a small amount of monomer were encapsulated in microemulsion micelles. A reducing agent was used to react with the Cu(II) complex and to generate the activator to initiate the polymerization. The rest of the monomer was gradually fed to the polymerization system. Small polymer particles and relatively narrow molecular weight distributions were expected.

## Chapter 3

### Experimental

#### 3.1 Materials

All materials were used as received, unless otherwise stated (Table 3-1).

**Table 3- 1 List of materials used in this project**

Chemical		Description
Copper (II) bromide	CuBr <sub>2</sub>	99% Aldrich
Cetyltrimethylammonium bromide	CTAB	95% Aldrich
Polyoxyethylene(20) oleyl ether	Brij98	Aldrich
2,2'-azobis[2-(2-imidazolin-2-yl)propane] dihydrochloride	VA-044	Wako Chemicals
1-Pentanol	C <sub>5</sub> H <sub>12</sub> O	99+% Aldrich
Acetone	(CH <sub>3</sub> ) <sub>2</sub> CO	Fisher Scientific
Ethyl 2-Bromoisobutyrate	EBiB	98% Aldrich
L-Ascorbic Acid	C <sub>6</sub> H <sub>8</sub> O <sub>6</sub>	≥99%,Sigma
Sodium hydroxide	NaOH	>97%, Aldrich
Octadecylamine	C <sub>18</sub> H <sub>39</sub> N	Aldrich
2-picoyl chloride hydrochloride		Aldrich
Tetrahydrofuran	THF	>99%, Aldrich
Methanol	CH <sub>3</sub> OH	99.9%, Fisher Scientific
Aluminum Oxide	AlO <sub>2</sub>	Standard Grade Aldrich
Ethyl acetate	C <sub>4</sub> H <sub>8</sub> O <sub>2</sub>	Aldrich
Nitrogen	N <sub>2</sub>	Ultra high purity, Praxair
De-ionized water	DIW	Distilled water purified by Milli-Q plus (a Millipore ultra-pure water system).

The n-butyl methacrylate (BMA, Aldrich) and n-butyl acrylate (BA, Aldrich) were purified by passing each through a column packed with inhibitor remover (Aldrich). THF for gel permeation chromatography (GPC) was distilled over calcium hydride under nitrogen atmosphere.

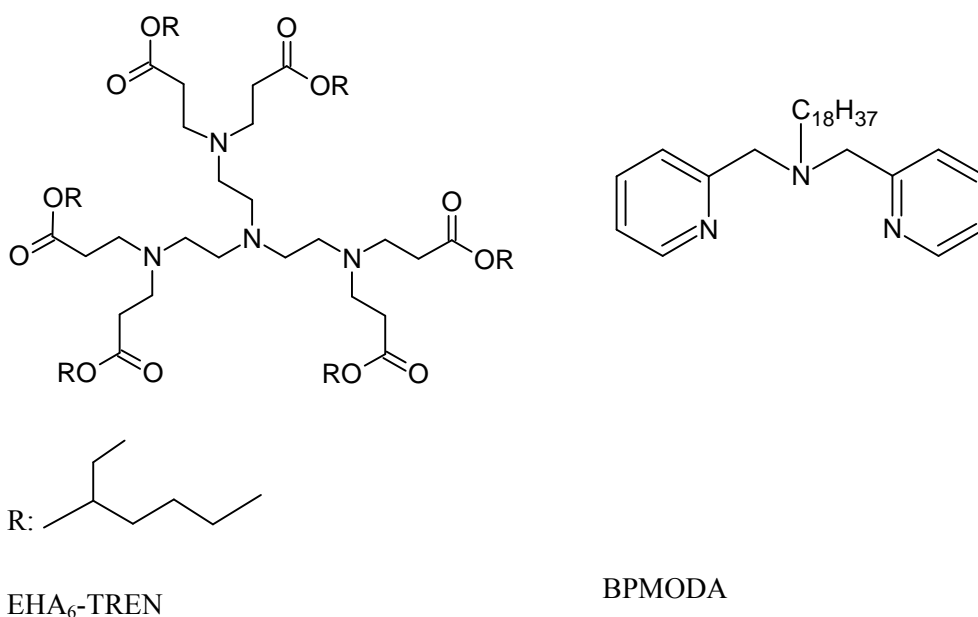


**Figure 3- 1 Structures of EHA<sub>6</sub>-TREN and BPMODA**

### Synthesis of Ligands

The synthesis of ligands of BPMODA<sup>(35)</sup> and Tris[2-di(2-ethylhexylacrylate)aminoethyl]amine (EHA<sub>6</sub>-TREN)<sup>(36,37)</sup> were adapted from the literature. To synthesize BPMODA, NaOH (2.5 g) in 100 mL deionized water, octadecylamine (4.0 g, 15 mmol), 2-picolyl chloride hydrochloride (5.0 g, 30 mmol), and THF (100 mL) were mixed and stirred at 50°C for 2 days. After being cooled down to the room temperature, a brown organic phase was collected. The brown organic phase was vaporized under a vacuum Rotovap at 125 rpm and 40°C for 2 h to remove the solvent and passed through a silica gel column. A brown mixture was collected by eluting with 1:1 methanol/ethyl acetate. BPMODA was obtained by removing the elution solvent under the

Rotovap for 5 hr. EHA<sub>6</sub>-TREN used in this experiment was synthesized freshly in our lab following the literature. The structures of EHA<sub>6</sub>-TREN and BPMODA are shown in Figure 3-1.

## 3.2 Analysis

### 3.2.1 Conversion

Gravimetry was used to determine the conversion of all samples. Each sample was weighed into a glass vial, air dried for a day, and then kept at 50°C under vacuum for 4 hr. It was assumed that water and monomer evaporate. From the formulation of the reaction, the mass fraction of each component could be calculated. Given the initial amount of monomer present, taking the amount of monomer converted to be that of the polymer in the dried sample, conversion can be calculated.

### 3.2.2 Gel Permeation Chromatography (GPC)

The molecular weight and polydispersity were obtained with gel permeation chromatography (GPC), which was performed using a Waters 2960 Separation Module. Four Styragel columns of pore sizes 100, 500, 10<sup>3</sup> and 10<sup>4</sup> Å were coupled with a differential refractive index detector maintained at 40°C. Flow rate of the eluant, tetrahydrofuran (THF), was set at 1.0 mL/min. Polystyrene (PS) standards were used for calibration. The universal calibration can be used to correct the molecular weights obtained for polystyrene to poly(butyl acrylate) and poly(butyl methacrylate). The Mark-Houwink parameters for polystyrene are  $K = 1.14E-04 \text{ dL}\cdot\text{g}^{-1}$  and  $\alpha = 0.716^{(53)}$ , and for poly(butyl acrylate)  $K = 1.22E-04 \text{ dL}\cdot\text{g}^{-1}$ ,  $\alpha = 0.7^{(55)}$ , and for poly(butyl methacrylate)  $K = 1.48E-04 \text{ dL}\cdot\text{g}^{-1}$ ,  $\alpha = 0.664^{(54)}$ . Dried polymer samples were dissolved in tetrahydrofuran (THF) and passed through a column packed with aluminum oxide to remove the residual copper.

### **3.2.3 Capillary Hydrodynamic Fractionation (CHDF)**

The particle size of the latexes was measured using a Capillary Hydrodynamic Fractionation (CHDF) 2000 unit produced by Matec Applied Sciences. The system was calibrated with 6 Seradyn Uniform Microparticle standards give sizes. The eluant was a 20 : 1 mixture of de-ionized water (DIW) and GR500-1X by Matec Applied Sciences. Samples have to be diluted by the eluant before passing through a 0.45  $\mu\text{m}$  pore size filter prior to injection.

### **3.2.4 Dynamic Light Scattering (DLS)**

The Zeta-Sizer Nano-ZS (Malvern) was also used to measure particle size; using Dynamic Light Scattering (DLS) with size range of 0.6 nm to 6  $\mu\text{m}$  and setup detector position at 173°. Samples were diluted before measuring. The intensity distributions display the result as intensity based particle size distribution. Large particles scatter much more light than small particles, and the intensity of scattering of a particle is proportional to the sixth power of its diameter (from Rayleigh's approximation). The volume distributions display the result as a volume based particle size distribution.

## **Chapter 4**

### **Atom Transfer Radical Polymerization (ATRP)**

In Chapter 2, various polymerization methods on the preparation of polymer nanoparticles were summarized. Since the differential microemulsion polymerization by He's group <sup>(1;2)</sup> showed advantages in reducing the concentration of surfactant in microemulsion, the focus of the present research is on developing a differential approach to prepare small nanoparticles in a controlled polymerization system. In this section, the differential method was applied to test for the feasibility of producing small nanoparticles with low surfactant concentration in ATRP.

#### **4.1 Conventional microemulsion polymerization**

He synthesized particles less than 20 nm in diameter by differential microemulsion polymerization <sup>(1;2)</sup>. The experiments were conducted for the monomers methyl methacrylate (MMA) and styrene. Anionic surfactant sodium dodecyl sulfate (SDS) and water soluble initiator ammonium persulfate (APS) were used in their experiments. This process provides a new method for preparing nano-sized polymer particles using much less surfactant than traditional microemulsion polymerization.

In this work, the differential microemulsion polymerization method was first employed in a traditional polymerization with butyl methacrylate (BMA) as the monomer and CTAB as the surfactant. CTAB is a cationic surfactant and will be used in the following ATRP experiments

##### **4.1.1 Experimental procedure**

In this differential microemulsion polymerization process, VA-044 was used as the initiator and CTAB as the surfactant. The initiator (VA-044, 0.0889 g) was dissolved in 2 mL of de-ionized water (DIW) deoxygenated by purging with nitrogen for 20 min. CTAB (1.25 g, 10 wt% vs.

monomer) and DIW (84 mL) were put into a three-neck flask equipped with a magnetic stirrer and a reflux condenser. After the temperature was raised to 65°C, the initiator was injected into the solution. Simultaneously, BMA (14 ml) containing 1-pentanol (0.2 ml) was added drop-wise to the flask over a period of about one and half hours. After the addition of the monomer, the reaction was kept at 65°C for one more hour.

#### **4.1.2 Results and discussion**

In this work, the surfactant / monomer ratio was about 1:10 (w/w), which is very low comparing to the traditional microemulsion in the literature. The polymerization rate was very fast, the conversion reached to 100% at the end of polymerization in about two hours. The final latex was transparent, indicating a very small particle size. By CHDF measurement, the mean particle size ( $D_n$ ) was 37.5 nm. The results showed that the cationic surfactant CTAB was promising to form nanoparticles in differential microemulsion polymerization.

#### **4.2 ATRP in microemulsion polymerization**

Living/controlled radical polymerization (L/CRP) techniques have been successfully used to synthesize polymers with predetermined molecular weight and narrow molecular weight distributions. Atom transfer radical polymerization (ATRP) is one of these techniques; ATRP has been successfully applied in emulsion and miniemulsion systems <sup>(5,38)</sup>. Particle size of approximately 130 nm was obtained in miniemulsion systems <sup>(14;15)</sup>.

In our research, differential method was applied to ATRP microemulsion to synthesize nanoparticles with controlled molecular weight and narrow polydispersity.

#### 4.2.1 Experimental procedure

Copper (II) bromide ( $\text{CuBr}_2$ , 0.059 g, 0.26 mmol), tris [2-di (2-ethylhexylacrylate) aminoethyl] amine ( $\text{EHA}_6\text{-TREN}$ , 0.30 g, 0.24 mmol), and butyl methacrylate (BMA, 0.058 g, 0.41 mmol) were added into a beaker and stirred overnight at room temperature to form the organic phase. The organic solution was then added to the surfactant solution consisting of cetyltrimethylammonium bromide (CTAB, 1.21 g) and deionized water (DIW, 84 mL), and stirred for approximately 30 min. The flask was immersed in an oil bath preheated to  $75^\circ\text{C}$ . The water soluble initiator 2, 2'-azobis [2-(2-imidazolin-2-yl) propane] dihydrochloride (VA-044, 0.048 g, 0.15 mmol) was dissolved in 2 mL of deionized water, and purged with nitrogen for 20 min prior to injecting into the system. After the initiation of the polymerization, the predeoxygenated mixture of BMA (14 mL, 0.088mol) and 1-pentanol (0.2 mL, 1.84 mmol) was added drop-wise over a period of one and half hours. Samples were withdrawn at regular intervals and placed in an ice bath before analysis.

#### 4.2.2 Results and discussion

A summary of experiments is shown in Table 4-1. No polymer was produced in the experiment conducted at  $60^\circ\text{C}$  (Exp. 1), even after five hours polymerization, probably because the reaction temperature was too low. After increasing the temperature to  $90^\circ\text{C}$  (Exp. 2), a slow polymerization rate was observed, and 40% conversion was achieved after six hours polymerization. Phase separation was observed in the final latex, probably because of the residual monomer due to the low conversion. Molecular weight values were much higher than the theoretical values and polydispersities were greater than 2, indicating a non-controlled polymerization (Figure 4-1).

In Exp. 3, a high initiator versus copper ratio and lower temperature was used. A fast polymerization rate was observed. The conversion was over 40% after half an hour, and then

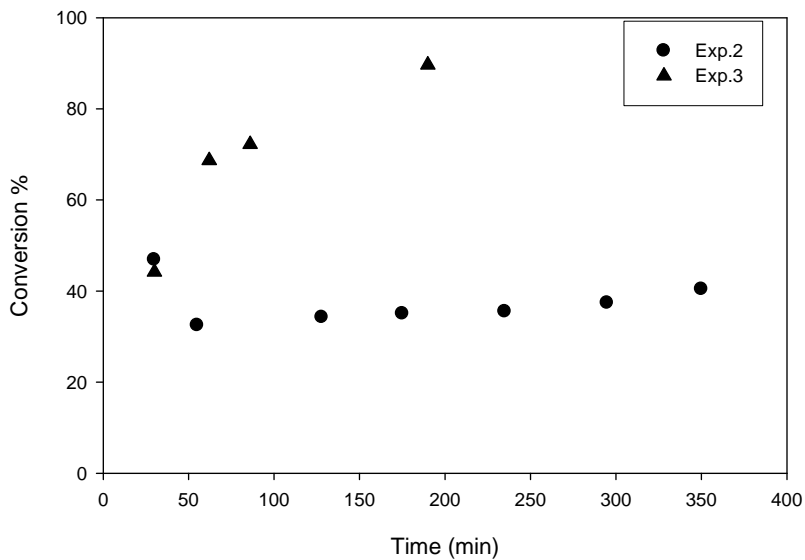
reached 90% after three hours. Polydispersity was high (over 2), indicating poor control although the polydispersity was decreasing with time. No phase separation was observed in the final latex, and particle size ( $D_n$ ) was 17.1 nm as measured by CHDF. In these microemulsion polymerizations, free radicals in aqueous phase must transfer to monomer droplets containing the catalyst species to function. However, micelles were formed in the solution due to a relatively high concentration of surfactant. Micelles were much smaller than the monomer droplets and were easier for the radicals to move into. The uncontrolled polymerization suggested that most of the radicals were captured by micelles (which do not contain catalyst) rather than the monomer droplets which do contain the catalyst species. Micellar nucleation result in non-controlled polymers with high molecular weights.

**Table 4- 1 Experimental conditions and results of BMA ATRP in microemulsion**

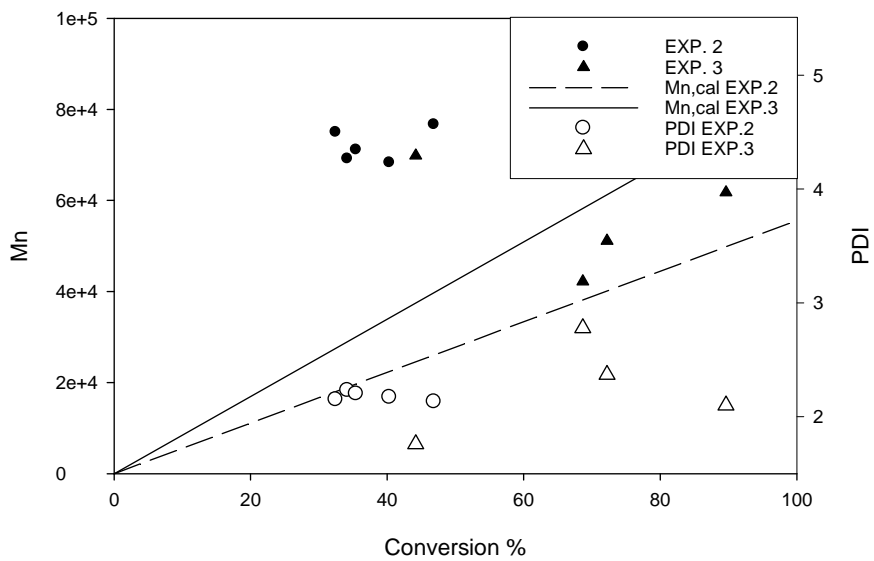
	[BMA]/[CuBr <sub>2</sub> ] /[VA-044]	CTAB <sup>a</sup> wt %	Temp. °C	Conv. %	Time min	M <sub>n,GPC</sub> (g/mol)	M <sub>n,cal</sub> (g/mol)	PDI
1	122/1/0.29	10	60	N/A	N/A	N/A	N/A	N/A
2	102/1/0.26	10	90	40.35	350	68282	55588	2.2
3	332/1/0.56	10	75	89.63	190	61731	84872	2.1

<sup>a</sup> [CTAB] = 10 wt% vs. monomer [BMA]

Overall, direct applying the differential method to ATRP in microemulsion polymerization was not successful. It is likely that those micelles (which do not contain catalyst) effectively compete with monomer droplets in capturing radicals. Secondary nucleation occurred, resulting in non-controlled polymerization, although stable nano-particles were obtained at the end of polymerization.



(a)



(b)

**Figure 4- 1 (a) conversion vs. time curve of conversion and (b) Mn vs. conversion in BMA ATRP microemulsion**

$[BMA]/ [CuBr_2]/ [VA-044] = 102/1/0.26$  and  $332/1/0.56$ ,  $[CTAB]/ [BMA] = 10$  wt%

### **4.3 Seeded microemulsion polymerization**

A seeded polymerization was considered to ensure that the catalyst-containing monomer droplets were the nucleation loci. Addition monomer was able to diffuse to these nucleation loci to complete the polymerization. An important concern in seeded polymerization was the secondary nucleation (micellar nucleation) which competed with monomer droplets to capture radicals and lead to non-controlled results. Chern et al. <sup>(39)</sup> studied the occurrence of secondary nucleation (micellar nucleation) under the monomer starved conditions (meaning that the water phase is not saturated with monomer). In their study, a second crop of particles was formed whenever micelles appeared in the reactor, and a bimodal particle size distribution was produced. Sajjadi <sup>(40)</sup> also studied the particle formation and coagulation in seeded emulsion polymerization under monomer starved conditions. Monomer addition rate controlled the secondary nucleation. The higher the concentration of monomer in aqueous phase, the larger was the number of secondary particles. Therefore, the addition rate of monomer must be very slow to ensure that no monomer droplets were formed.

In this research, a series of experiments were conducted in seeded microemulsion polymerization to produce nanoparticles with predetermined molecular weight and narrow polydispersity.

#### **4.3.1 Experimental Procedure**

##### **Making seeds by conventional microemulsion polymerization**

The initiator (VA-044, 0.08 g) was dissolved in 2 mL of DIW, deoxygenated by purging with nitrogen for 20 min. CTAB (CTAB, 1.26 g) and de-ionized water (DIW, 85mL) were mixed in a flask and put into a oil bath preheated to 65°C. Then the initiator was injected into the solution and BMA (1 mL) was added drop-wise over a period of about 10 min. The start of the feeding step and the addition of the initiator occurred simultaneously. After completion of monomer

addition, the reaction temperature was kept at 65°C for one hour before cooling to ensure a high monomer conversion.

### **Seeded ATRP Microemulsion Polymerization**

Copper (II) bromide ( $\text{CuBr}_2$ , 0.066 g), tris[2-di(2-ethylhexylacrylate)aminoethyl]amine ( $\text{EHA}_6\text{-TREN}$ , 0.32 g), and butyl methacrylate (BMA, 0.35 g) were added into a beaker to form the organic phase and stirred overnight at room temperature. The organic solution was then transferred to the seed latex made at the first step and stirred overnight at room temperature. The solution was purged by nitrogen for 30 min and then immersed in an oil bath preheated to the designated temperature. The water soluble initiator 2, 2'-azobis [2-(2-imidazolin-2-yl) propane] dihydrochloride (VA-044, 0.044 g) was dissolved in 2 mL of deionized water, and purged with nitrogen for 20 min prior to injection into the system. After the initiation step, the predeoxygenated mixture of BMA (14 mL) and 1-pentanol (0.2 mL) was added drop-wise over a period of one and half hours. Samples were withdrawn at regular intervals and placed in an ice bath before analysis.

### **Acetone as phase transfer agent**

Seed latex was prepared using the same procedure as described above. Copper (II) bromide ( $\text{CuBr}_2$ , 0.066 g), tris[2-di(2-ethylhexylacrylate)aminoethyl]amine ( $\text{EHA}_6\text{-TREN}$ , 0.32 g), and butyl methacrylate (BMA, 0.35 g) were added into a beaker to form the organic phase and stirred overnight at room temperature. Acetone solution consisting of acetone (20 g) and DIW (84 mL) was added to the seed latex made in the first step and stirred for four hours under nitrogen. The organic solution was transferred into this mixture and stirred overnight under nitrogen. The mixture was then heated to 58°C to evaporate acetone for one hour. Then the flask was immersed in an oil bath preheated to the designated temperature. The water soluble initiator 2, 2'-azobis [2-

(2-imidazolin-2-yl) propane] dihydrochloride (VA-044, 0.051 g) was dissolved in 2 mL of deionized water, and purged with nitrogen for 20 min prior to injection into the system. After the initiation step, the predeoxygenated mixture of BMA (14 mL) and 1-pentanol (0.2 mL) was added drop-wise over a period of one and half hour. Samples were withdrawn at regular intervals and placed in an ice bath.

### 4.3.2 Results and discussion

All seeds were made by conventional microemulsion polymerization, and very high conversions were obtained in the seed latex. Exp. 4, 5, and 6 were conducted by the seeded ATRP microemulsion polymerization and Exp. 7 and 8 were conducted by the acetone-assisted-phase-transfer seeded ATRP microemulsion polymerization (Table 4-2). In all experiments, low surfactant concentration was used to avoid the presence of micelles in the seed latex and the addition rate of monomer was very slow to ensure that no monomer droplets were formed and no droplet nucleation occurred

**Table 4- 2 Experimental conditions and results of BMA in seeded ATRP microemulsion polymerization**

	Conv. Seed <sup>a</sup> %	[BMA]/[CuBr <sub>2</sub> ] /[VA-044]	CTAB <sup>b</sup> wt %	Tem. °C	Conv. %	Time min	M <sub>n,GPC</sub> (g/mol)	M <sub>n,cal</sub> (g/mol)	PDI
4	88.69	118/1/0.34	7.85	75	5.1	345	multiple peaks		
5	97.86	296/1/0.46	9.04	70	8.78	284	long tail		
6	100	352/1/0.55	8.37	70	98.56	185	48792	91746	1.94
7	88.38	370/1/0.67	4.34	65	90.53	202	62455	79039	2.16
8	92.42	387/1/1.01	5.73	80	56.49	120	27637	54465	2.49

<sup>a</sup> final conversion of seed latex

<sup>b</sup> [CTAB] vs. [BMA] by weight

Exp. 4 and 5 showed very slow polymerization rates and low final conversions (Figure 4-2). In Exp.6, a lower concentration of copper and higher concentration of initiator were applied, leading to a fast reaction rate (99% conversion was obtained) and a small particle size of 39.6 nm as measured by CHDF. In Exps. 4 and 5, molecular weight distribution was not unimodal, and a broad molecular weight distribution was observed in Exp. 6, indicating non-controlled polymerizations.

In this seed polymerization, the seed polymer particles were swollen by monomer containing catalyst species so that the catalyst species were present only in the pre-existing seed polymer particles in ideal conditions. However, phase transfer of the catalyst to the polymer particles was difficult due to the large size and high hydrophobicity of the catalyst. The difficulties of achieving uniform catalyst distribution within the particles resulted in the poor control of molecular weight and polydispersity in this seeded microemulsion polymerization.

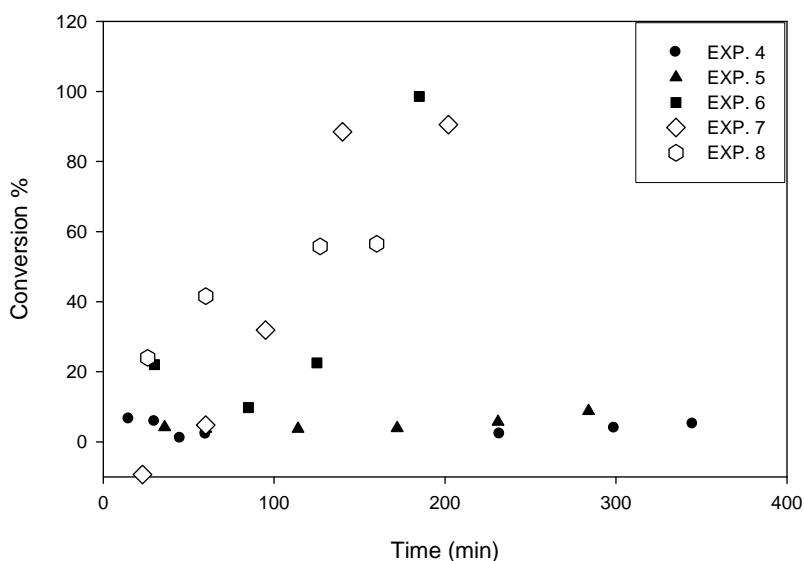


**Figure 4- 2 Conversion as a function of time of BMA in seeded ATRP microemulsion polymerization**

In order to overcome the catalyst transportation problem, acetone was used as a phase transfer agent to facilitate the transport of the catalyst from monomer droplets into the polymer particles in the seed polymerization. In Prescott's study<sup>(41)</sup>, acetone was used to localize RAFT agent in the particle phase in seeded emulsion polymerization of styrene, since acetone was able to transport hydrophobic species in the aqueous phase.

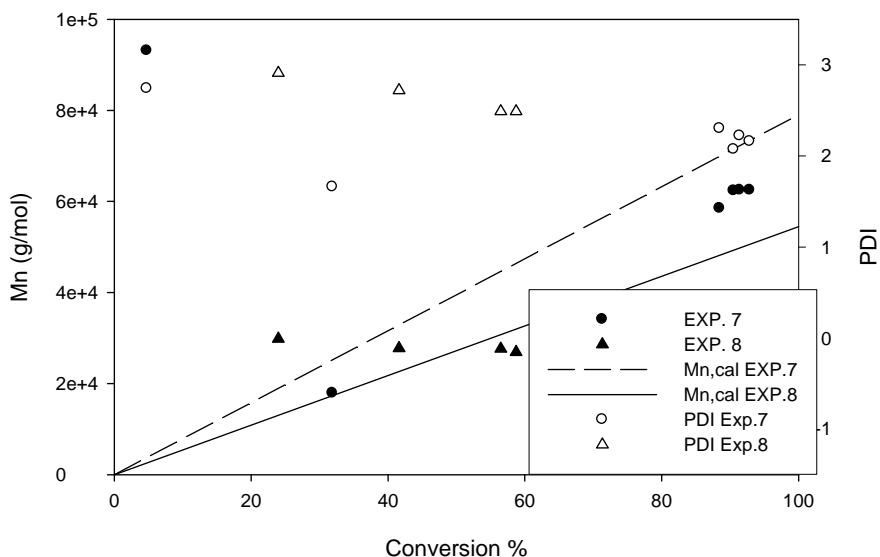


**Figure 4- 3 Evolution of molecular weight ( $M_n$ ) of BMA in seeded ATRP microemulsion polymerization by using acetone as transfer agent.**

**[BMA]/ [CuBr<sub>2</sub>]/ [VA-044] = 370/1/0.67 and 387/1/1.01, respectively. Reaction Temp = 65°C and 80°C.**

Acetone was used as a phase transfer agent in Exp. 7 and 8. Exp.7 was a semi-batch operation (monomer was added into the seeded latex continuously), and Exp. 8 was a batch polymerization (all monomers were used to dissolve catalyst at the outset). Fast polymerization rates were observed in both experiments. However, in the batch process (Exp. 8) conversion stopped at ~60 % while the conversion reached over 90 % in the semi-batch operation (Exp. 7) (Figure 4-2).

Very high initial molecular weight was observed in the semi-batch operation (Exp. 7), representing the seeds. As the polymerization progressed, experimental molecular weights were lower than the theoretical values, indicating more propagating chains formed than expected. The polydispersity was high ( $>2$ ) as well. Some micelles might be present in the system resulting in micellar nucleation and non-controlled results.

In the batch operation (Exp. 8), the experimental molecular weight increased linearly as a function of conversion. Although the initial value was higher than the theoretical value, the molecular weight agreed fairly well with the theoretical values in the later polymerization. The polydispersity decreased over the course of polymerization, although it was still quite high ( $>2$ ) at the end of polymerization (Figure 4-3). In the batch operation, the locus of polymerization was the seed latex particles which were swollen by the monomer and the catalyst. However, some monomer droplets were present in the system simultaneously, resulting in monomer droplet nucleation and broad polydispersity. Overall, the complexity of effectively distributing catalyst within the particles is the main problem in seeded ATRP microemulsion polymerization. Using acetone as a phase transfer agent improved the results somewhat, but did not solve the problem.

#### **4.4 Conclusion**

Conventional differential microemulsion polymerization was achieved by using a cationic surfactant, CTAB, with the low weight ratio of surfactant/monomer (1:10). Particles with a mean diameter of less than 40 nm were obtained in this system. Smaller particles were obtained in ATRP microemulsion, but unfortunately poor controlled polymerization was obtained. Particle formation mechanism was too complex leading to poor controlled results in seeded microemulsion polymerization. When acetone was used as a phase transfer agent to assist transport of the large catalyst molecules into particles in seeded microemulsion polymerization, improved results were obtained.

## Chapter 5

### Generating Nano-sized PolyButyl Acrylate using AGET ATRP

#### 5.1 Introduction

Atom transfer radical polymerization (ATRP) provides a facile route to synthesize polymers with well-controlled molecular weight and narrow molecular weight distributions<sup>(42;43)</sup>. ATRP was successfully applied to emulsion and miniemulsion systems<sup>(5;14;38)</sup>. However, only one study was reported in a microemulsion system. In Min's study, better results were obtained from AGET ATRP than from either normal ATRP or reverse ATRP in microemulsion when methyl methacrylate (MMA) was used as monomer, polyoxyethylene(20) oleyl ether (Brij98) as surfactant, and Bis (2-pyridylmethyl) octadecylamine (BPMODA) as ligand<sup>(22)</sup>. The average diameter particle size was 43 nm and polydispersity was 1.28. However, the weight ratio of surfactant to monomer was very high ([surfactant]/ [MMA] ~2.5), which is a common problem in microemulsion. He et al. reported the synthesis of poly methyl methacrylate (PMMA) nanoparticles and polystyrene using differential microemulsion polymerization, which is based on a semi-continuous microemulsion polymerization<sup>(1; 2)</sup>. A small amount of monomer was added into the reactor first, and then the remaining monomer was added in a differential manner (continuous addition in very small drops). The PMMA particles obtained were less than 20 nm with a low weight ratio of surfactant/monomer of 1:18. However, both studies were based on traditional polymerization and molecular weight and the molecular weight distribution were not controlled. In another study by Matyjaszewski's group, AGET ATRP was successfully adapted in an ab initio emulsion polymerization by using n-butyl acrylate as monomer, Brij98 as surfactant and BPMODA as ligand<sup>(44)</sup>. A controlled ab initio emulsion polymerization with narrow molecular weight distribution ( $M_w/M_n=1.2\sim 1.4$ ) was obtained, but the final particle size in the latex was ~100 nm. The synthesis of a small sized polymer (~50 nm) in a low surfactant/monomer ratio was not reported in a controlled polymerization.

In this study, we demonstrate the feasibility of producing nanoparticles (particle size < 50 nm) with controlled molecular weight and narrow molecular distribution in a low surfactant microemulsion system using AGET ATRP. In our two-step differential AGET ATRP, all initiators, catalysts, and a small amount of monomer were mixed to form an initial microemulsion in the first stage, and the rest of the monomer was continuously added into this polymerization system as droplets after the initiation reaction. The cationic surfactant cetyltrimethylammonium bromide (CTAB) was used.

## **5.2 Experimental**

### **Materials**

n-Butyl acrylate (BA, Aldrich) was purified by passing through a column packed with inhibitor remover (Aldrich). The compounds copper (II) bromide ( $\text{CuBr}_2$ , 99 % Aldrich), cetyltrimethylammonium bromide (CTAB, 95 % Aldrich), polyoxyethylene (20) oleyl ether (Brij98, Aldrich), ethyl 2-Bromoisobutyrate (EBiB, 98 % Aldrich), L-Ascorbic Acid ( $\text{C}_6\text{H}_8\text{O}_6$ , 99 %, Sigma) were used as received. The synthesis of BPMODA was adapted from literature<sup>(35)</sup>.

### **AGET ATRP in microemulsion polymerization**

The organic phase was prepared by dissolving copper (II) bromide ( $\text{CuBr}_2$ , 0.0428 g, 0.19 mmol) and BPMODA (0.137 g, 0.30 mmol) in BA (5 ml) in a beaker and stirring overnight at room temperature to form a homogeneous solution. The initiator, ethyl 2-bromoisobutyrate (EBiB, 0.0757 g, 0.39 mmol), was then dissolved in this mixture. After stirring for 30 min, a one-fifth fraction of the mixture (0.9609 g) was taken out as the organic phase. The aqueous phase consisting of the surfactant cetyltrimethylammonium bromide (CTAB, 36 wt % vs. monomer) and deionized water (DIW, 30 mL) was stirred for 30 min before the organic phase was added. An initial microemulsion was formed by stirring for 60 min under nitrogen. The initial

microemulsion was then immersed in an oil bath that was preheated to 80°C. The reducing agent solution (0.5 ml) containing L-ascorbic acid (2.6 mg) was purged with nitrogen for 20 min and injected into the initial microemulsion with a deoxygenated syringe to initiate the polymerization. After polymerizing for five minutes, the predeoxygenated second part of BA (2 mL) was added drop-wise to the microemulsion over 20 min, and typically 4 more hours were required to complete the polymerization. Samples were taken at regular intervals and placed into an ice bath before analysis.

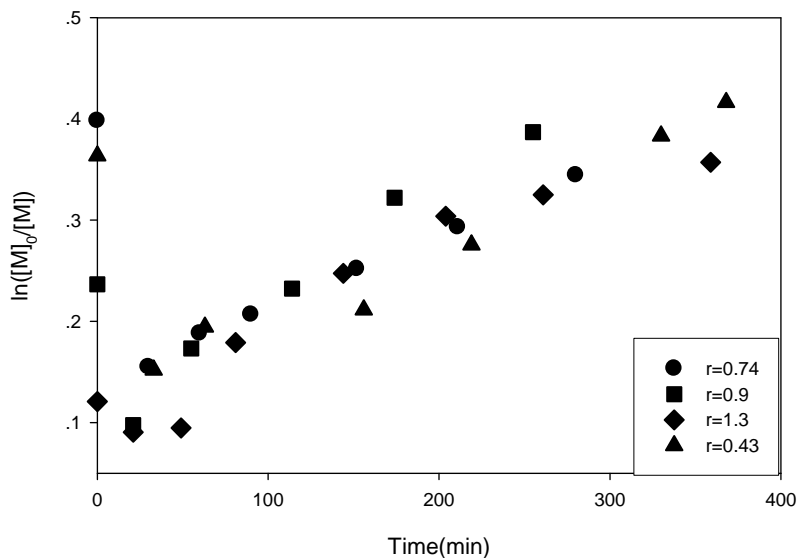
### **Characterization**

Monomer conversions were determined gravimetrically. Gel permeation chromatography (GPC) was used to measure the molecular weight and polydispersity of the polymer samples. Dried polymer samples were dissolved in tetrahydrofuran (THF) and passed through a column packed with aluminum oxide to remove the residual copper. The GPC was performed using a Waters 2960 Separation Module with four Styragel columns of pore sizes 100, 500, 10<sup>3</sup> and 10<sup>4</sup> Å. Flow rate of the eluant, THF, was set at 1.0 mL/min. Polystyrene standards were used for calibration. The Zeta-Sizer Nano-ZS (Malvern) was used to measure particle sizes using Dynamic Light Scattering (DLS).

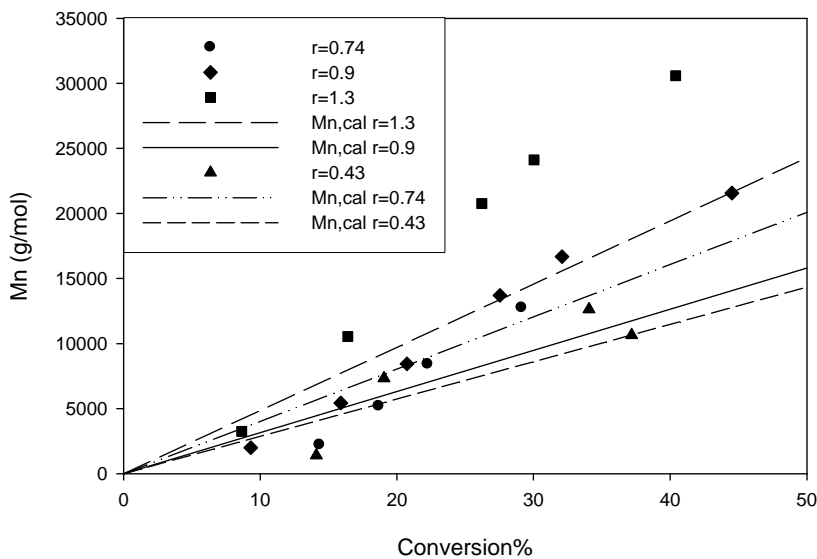
## **5.3 Results and Discussion**

### **5.3.1 Effect of the catalyst concentration**

Since the catalyst controls the dynamic equilibrium between dormant species and propagating radicals, it plays a very important role in ATRP. To determine a suitable catalyst concentration, four different levels of catalyst, 0.43, 0.74 to 0.9 and 1.3 (equiv vs. initiator, mol/mol) were investigated.



(a)



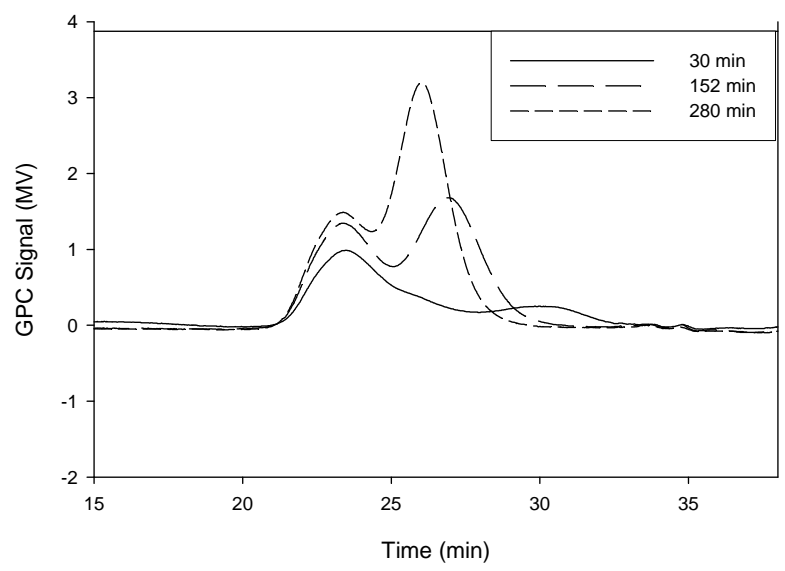
(b)

**Figure 5- 1 Effect of catalyst concentration on BA polymerization (a) First-order kinetic plots (b) Evolution of Molecular weight versus conversion.**

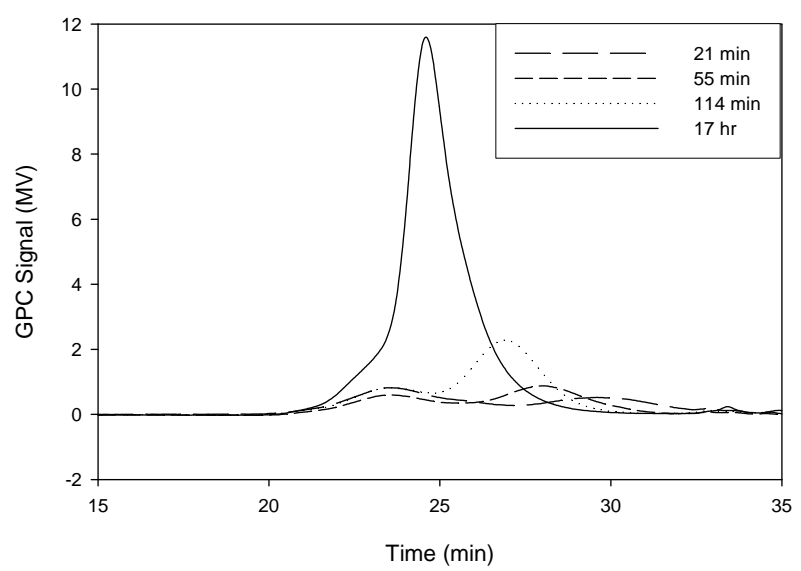
**[CuBr<sub>2</sub>]: [EBiB] = r = 1.3, 0.9, 0.74, and 0.43, respectively, Reaction temp = 80°C, [CuBr<sub>2</sub>]: [ascorbic acid] = 2.5, [CTAB] = 37 wt % vs. monomer**

As shown in Figure 5-1 (a), the catalyst concentration had significant effect on the initial conversion; higher initial conversion was obtained at the low catalyst concentration and lower initial conversion was obtained at the high catalyst concentration. After the initiation, however, the conversion profiles were similar for all four concentrations. Molecular weights ( $M_n$ ) increased approximately linearly with conversion (Figure 5-1 (b)). For the two lowest catalyst concentrations ( $r = 0.43$  and  $0.74$ ), the experimental and theoretical values were in good agreement, but for the highest catalyst concentrations ( $r = 1.3$ ), the experimental  $M_n$  values was noticeably higher, indicating that fewer chains than expected were formed. For all experiments, the initial number of chains was higher than that at the end of the experiment implying the existence of either termination or a bias in the conversion measurements, possibly due to difficulties in accurately measuring conversion at low times in a semi-batch system. The higher catalyst concentration experiments also show curvature in the conversion plots, indicating a slow polymerization that suggests reduced concentration of propagating chains, which is consistent with termination.

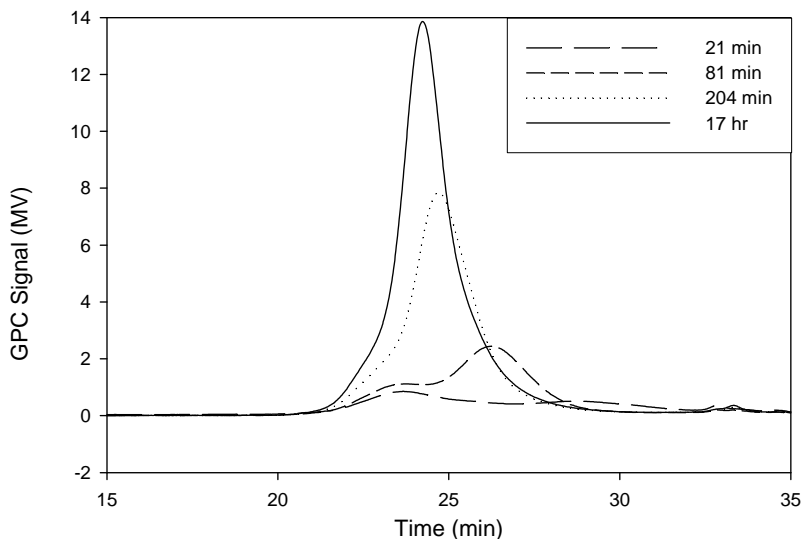
At the end of the polymerization, the conversion was less than 50%, even after overnight polymerization (data not shown). Theoretically, a controlled radical polymerization is governed by the persistent radical effect, so the system requires that some termination occur<sup>(45)</sup>. If the formation of deactivator as a persistent radical is much greater than the concentration of free radicals, polymerization will halt at low conversion<sup>(9)</sup>. The concentration of deactivator was likely much greater than the concentration of radicals over the course of the polymerization in the higher initial catalyst concentration experiments. In the lower catalyst concentration experiments, the concentration of deactivator was also greater than the concentration of radicals in the final latex due to the consumption of free radicals by termination in the initial stages of reaction.



(a)



(b)



(c)

**Figure 5- 2 Effect of catalyst concentration on GPC traces for AGET ATRP of BA in a microemulsion [CuBr<sub>2</sub>]: [EBiB] = r = 0.74 (a), 0.9 (b) and 1.3 (c)**

**(indicating time is polymerization time)**

In the GPC traces, growing peaks were clearly observed at all concentrations of catalyst. The particle size in the latex was less than 20 nm for all catalyst concentrations (Table 5-1), and the smaller particles were obtained from the lowest catalyst concentration. To the author's knowledge, this is the first report showing the feasibility of generating nano-sized polymers (< 20 nm) with the controlled molecular weight in a low surfactant microemulsion ATRP.

A high-molecular-weight peak was formed in the initial polymerization step, especially when the catalyst concentration was low ( $r = 0.74$ ) (Figure 5-2). At high catalyst concentrations, however, the high-molecular-weight peak was not significant in the end of the polymerization comparing to the growing peak. The possible reason for the forming of the dead high-molecular-weight peak was the lack of deactivator initially. The initial concentration of deactivator Cu(II) in the polymerization has to be sufficiently large to ensure a fast deactivation rate  $k_{\text{deact}}$ , otherwise the coupling of propagating radicals will occur leading to termination<sup>(9)</sup>. The number of Cu(II)

molecules in each particle can be significantly increased with the increase of the catalyst concentration leading to a better controlled polymerization (Table5-1). The initial catalyst concentration between 0.74 and 0.9 appears to be a good choice after the molecular weight, conversion, particle size and GPC results were considered. (The number of Cu(II) molecules in each particle was calculated by

$$\frac{A * n_{CuBr_2}}{n_{BA} / \left( \frac{4}{3} * \pi \left( \frac{D}{2} \right)^2 * \rho \right)}$$

Where  $n_{CuBr_2}$  and  $n_{BA}$  are moles of copper and monomer BA, respectively. A is Avogadro's number, D is diameter of polymer particles and  $\rho$  is the density of polymer.)

**(Mn values, for bimodal peaks, measured for the growing molecular peaks.)**

**Table 5- 1 The effect of catalyst concentration on particle size**

[Cu(II)]:[EBiB] r	Time min	Conversion (%)	Mn (g/mol)	M <sub>n,cal</sub> (g/mol)	Particle Size nm	No.CuBr <sub>2</sub> Per particle <sup>c</sup>	PDI <sup>d</sup>
0.43	368	35.06	12632	9768	9 (Dv) <sup>a</sup>	2.86	0.44
0.74	280	29.14	12739	11702	8 (Dv)	2.94	0.95
0.90	255	32.09	16673	10142	16 (Dz) <sup>b</sup>	39.4	0.39
1.30	359	30.04	24113	19620	20 (Dz)	67.5	0.63

<sup>a</sup> Dv- volume based particle size distribution measured by DLS

<sup>b</sup> Dz- Z-average mean diameter as an intensity based particle size distribution

<sup>c</sup> number of Cu(II) molecules in each particle

d: index of particle size distribution

The particle sizes of 9 and 8 nm refer to the Dv, because the samples were quite polydisperse and therefore the Dz measurements cannot be reliably determined. . The values were probably not accurate, but do indicate the formation of small particles (<~20 nm). (No peaks were visible by CHDF analyses, indicating the particles were smaller than ~35-40 nm). TEM images were obtained, but the images were blurry, possibly due to the low Tg of the polymer.

### 5.3.2 Effect of the surfactant concentration

In microemulsion polymerization, the amount of surfactant has a significant influence on the stability and the final polymer particle size. In this section, the effect of CTAB concentration on AGET ATRP was investigated at two different catalyst concentrations. Two surfactant concentrations were studied at low catalyst concentration (0.5), and three surfactant concentrations were studied at the high catalyst concentration (1.3).

The polymerization rate was high at the high surfactant concentration (68.8 and 68.7 wt %) and final conversion reached greater than 50 % as shown in Figure 5-3 (a). However, the final microemulsion showed non-controlled behavior due to this fast polymerization. Since the particle size was decreased with increasing surfactant concentration, and less Cu(II) can be present in the smaller particles (Table 5-2), the equilibrium was hard to build up in the high surfactant concentration resulting in loss of control. A sufficient amount of deactivating species (i.e. X-Cu(II)) is always needed for well-controlled polymerization since molecular weight distribution depends on the ratio of the propagation and deactivation rate constants and the concentration of deactivator<sup>(18)</sup>.

Experiments with relatively lower concentration of surfactant (37.2, 27.6, and 35.8 wt %) had similar conversion profiles, but final conversions were all lower than 50 %. The measured molecular weight differed from the theoretical value (Figure 5-3 (b)) at the high surfactant concentration (37.2 %) indicating lower initiator efficiency. At the lower surfactant concentration, larger particles were formed. Therefore, relatively more Cu(II) deactivator was present in each particle and the ATRP equilibrium was built up quickly leading to better control.

**Table 5- 2 Experimental conditions and results for AGET ATRP of BA microemulsion polymerization on effect of surfactant concentration**

[CuBr <sub>2</sub> ]:[EBiB] r	[CTAB]:[BA] (R) wt%	Time (min)	Conversion %	M <sub>n, GPC</sub> (g/mol)	M <sub>n, Cal</sub> (g/mol)	Particle size <sup>a</sup> nm	No. Cu(II) per particle <sup>b</sup>	PDI <sup>d</sup>
0.5	68.8	259	39.71	31990	18987	N/A	N/A	
	35.8	368	34.06	12632	9769	9 (D <sub>v</sub> )	2.86	0.44
1.3	68.7	311	77.98	20571	38771	13 (D <sub>v</sub> )	20.3	0.74
	37.2	354	30.04	24113	19620	20 (D <sub>z</sub> ) <sup>c</sup>	67.5	0.63
	27.6	242	28.09	19799	12778	22 (D <sub>v</sub> )	86.9	0.46

<sup>a</sup> volume based particle size distribution measured by DLS

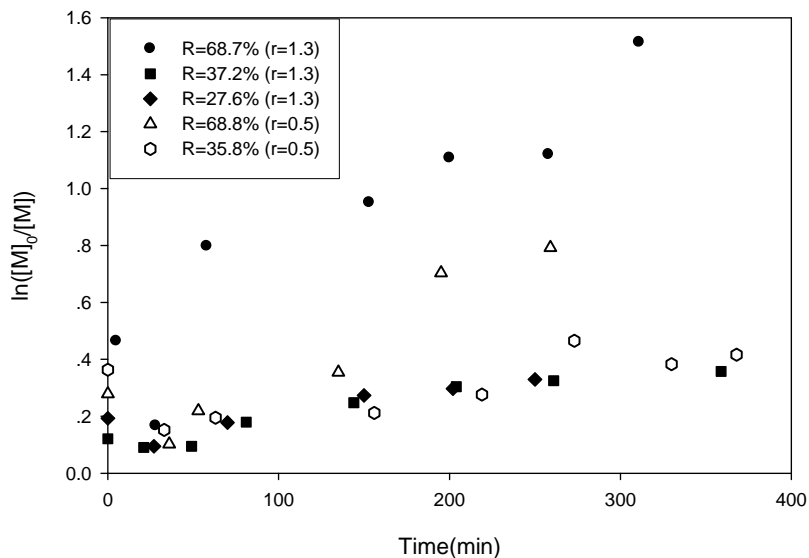
<sup>b</sup> number of Cu(II) molecules in each particle was calculated by

$$\frac{A * n_{CuBr_2}}{n_{BA} / \left( \frac{4}{3} * \pi \left( \frac{D}{2} \right)^2 * \rho \right)}$$

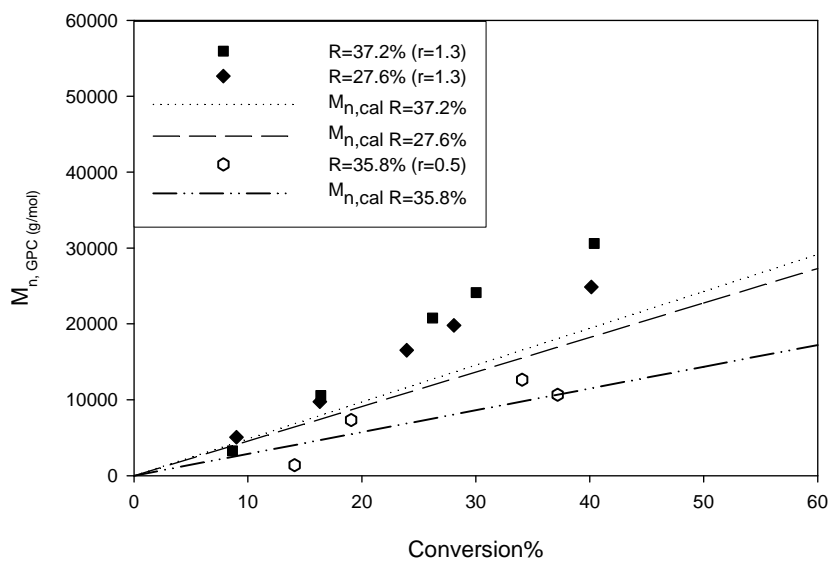
Where  $n_{CuBr_2}$  and  $n_{BA}$  are moles of copper and monomer BA, respectively. A is Avogadro's number, D is diameter of polymer particles and  $\rho$  is the density of polymer.

<sup>c</sup> Z-average mean diameter as an intensity based particle size distribution

<sup>d</sup> index of particle size distribution



(a)

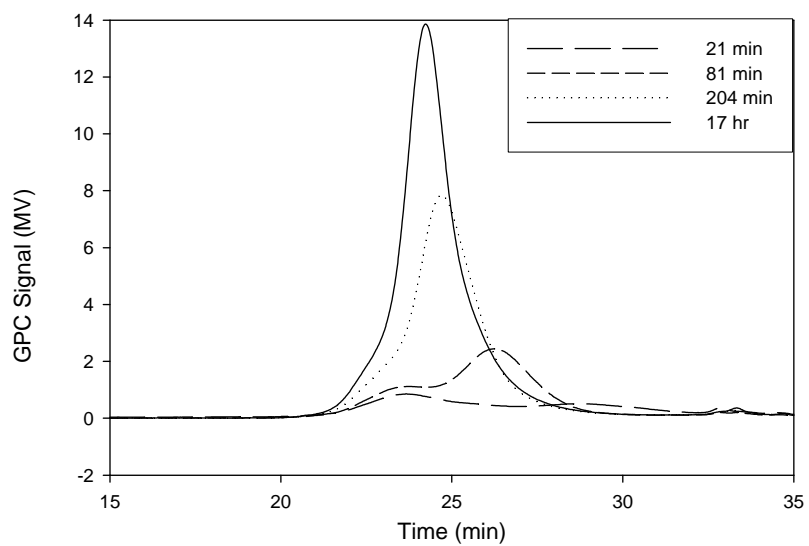


(b)

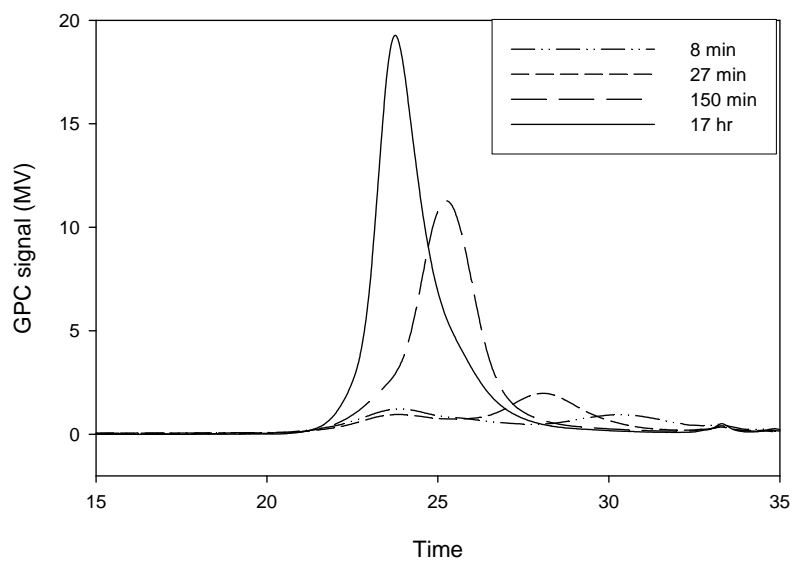
**Figure 5- 3 Effect of surfactant concentration on BA polymerization (a) first-order kinetic plots and (b) evolution of Mn**

**[CuBr<sub>2</sub>]: [EBiB] = r = 0.5, 1.3, respectively and R is the different ratios of [Surfactant]: [BA]**

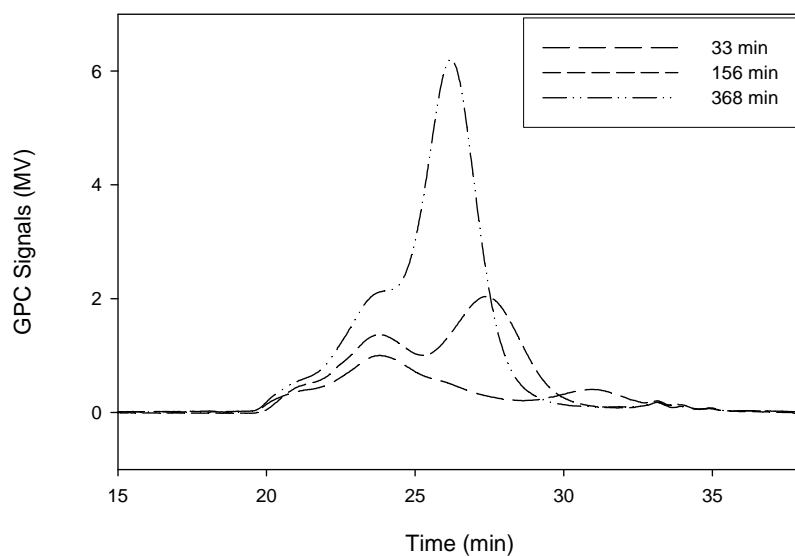
**Reaction temp = 80°C, [CuBr<sub>2</sub>]/[ascorbic acid] = 2.5**



(a)



(b)



(c)

**Figure 5- 4 GPC traces on the effect of surfactant concentration on BA AGET ATRP [CTAB]/ [BA] (wt %) equals to (a) 37.2 (b) 27.6 and (c) 35.8**

**[CuBr<sub>2</sub>]/ [EBiB] = 1.3 in (a) and (b), [CuBr<sub>2</sub>]/ [EBiB] = 0.5 in (c) Reaction Temp = 80°C (indicating time is polymerization time)**

In the GPC traces (Figure 5-4), bimodal peaks again showed up in the beginning, and the living low molecular weight grew with time. Subsequently, one broad peak appeared instead of bimodal peaks over the course of polymerization.

### 5.3.3 Effect of surfactants (CTAB vs. Brij98)

Nonionic surfactant stabilizes the latex by thermodynamically favorable steric interactions and becomes less effective as the temperature rises <sup>(15)</sup>. In contrast to nonionic surfactants, the stabilization of particles by ionic surfactant is mainly governed by electrostatic repulsion, and not dependent on temperature. Particles will not coagulate if the potential energy barrier exceeds the

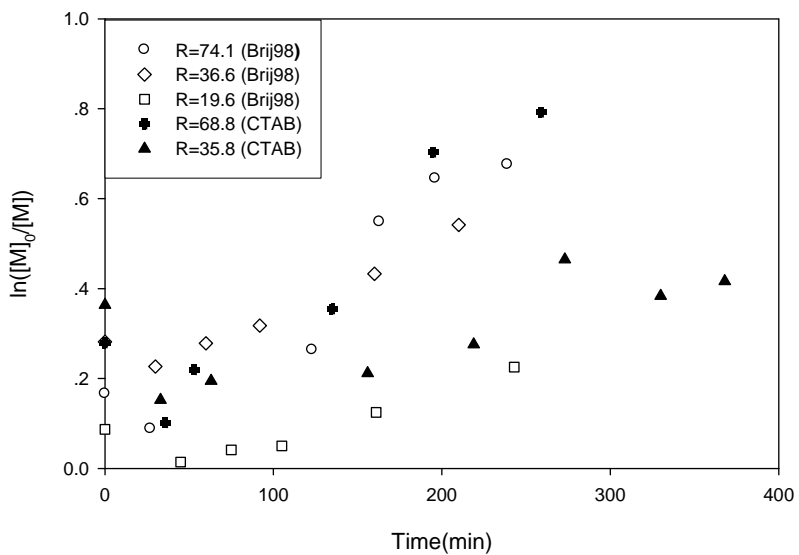
kinetic energy of particles. As surfactant molecules adsorb on the surface of particles, the electrostatic repulsion increases, resulting in more stable particles<sup>(40)</sup>. CTAB (cetyltrimethylammonium bromide) is a cationic surfactant and was adapted effectively to stabilize miniemulsion by reverse ATRP<sup>(15)</sup>. In this section, the effects of nonionic surfactants Brij98 and CTAB were compared in AGET ATRP BA microemulsion polymerization.

**Table 5- 3 The effect of Brij98 and CTAB on BA polymerization**

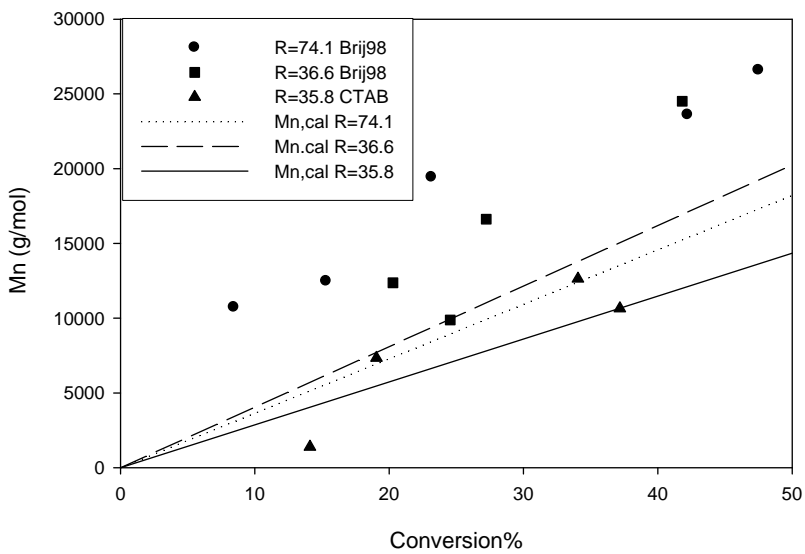
Surfactant	[surfactant]:[BA] wt%	Time (min)	conversion %	M <sub>n,GPC</sub> (g/mol)	M <sub>n,Cal</sub> (g/mol)	PDI	
BA	74.1	239	49.13	26580	17300	1.59	
	Brij98	36.6	210	41.82	24504	16925	1.49
	19.6	243	20.19	20004	7740	1.51	
	CTAB	68.8	259	39.71	31990	18987	bimodal
	35.8	368	35.06	12632	9769	bimodal	

[CuBr<sub>2</sub>]/ [EBiB] =0.5, Reaction temp =80°C.

(M<sub>n</sub> values, for bimodal peaks, measured for the growing molecular peaks.)



(a)



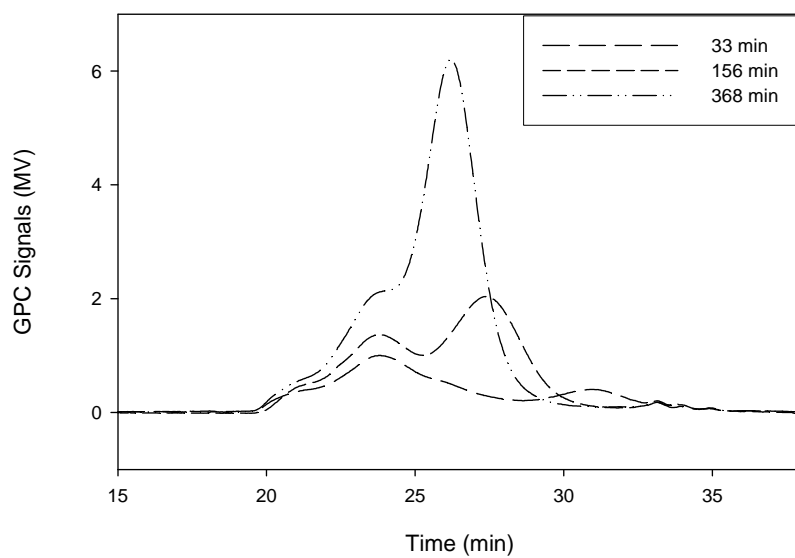
(b)

**Figure 5- 5 Comparison of Brij98 and CTAB on BA polymerization (a) conversion evolution and (b) molecular weight dependence  $[CuBr_2]/[EBiB] = 0.5$ ,**

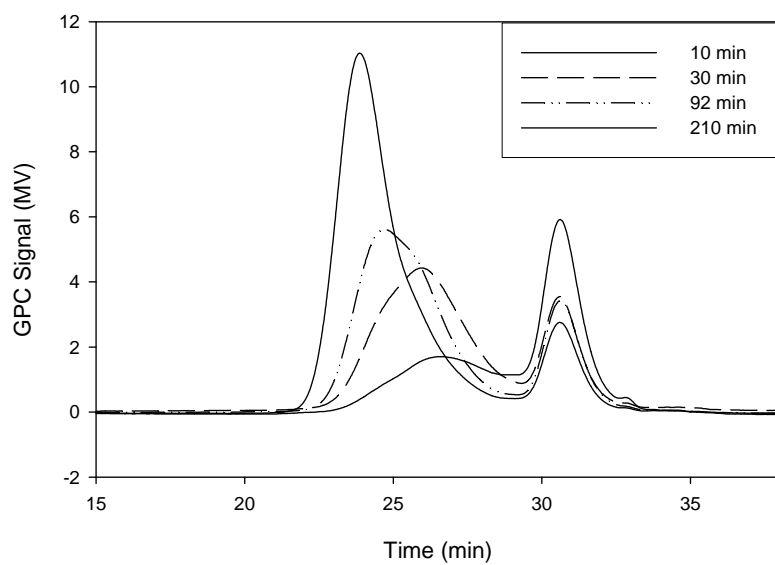
**Reaction temp = 80°C.**

As shown in Table 5-3, the polymerization rate increased with the increasing of surfactant concentration, in both Brij98 and CTAB. At similar surfactant concentrations the reaction rate was slower when CTAB was used (Figure 5-5 (a)). At a similar concentration (36.6 and 35.8 wt %), the system with CTAB exhibited better control in terms of better agreement of measured molecular weight with predicted values (Figure 5-5(b)). By DLS measurement, the particle size was 153.2 nm in Brij98 (36.6 wt %), and the particles size nm was only 8.7 nm in CTAB (35.8 wt %). (This value is probably not accurate, but it does indicate a very large difference in particle size between the two surfactants.)

In Figure 5-6 (b), that small molecular weight peak is the Brij98. By using Brij98 as surfactant only one growing peak was observed in the GPC traces, but bimodal peaks were present when CTAB was used (Figure 5-6 (a)). Since larger particles were formed in Brij98 than those in CTAB, more Cu(II) was present in Brij98 ( $1.57 \times 10^4$  (No. Cu / per particle)) than in CTAB (2.86 (No. Cu / per particle)). Therefore, the ATRP equilibrium was set up very quickly with Brij98, and there was no high-molecular weight peak initially. Overall, CTAB was able to form nanoparticles smaller than 20 nm and was feasible in AGET ATRP polymerization yielding a better controlled polymerization.



(a)



(b)

**Figure 5- 6 Comparison of Brij98 and CTAB on GPC traces (a) [CTAB]: [BA] = 35.8 wt %, (b) [Brij98]: [BA] = 36.6 wt %, [CuBr<sub>2</sub>]: [EBiB] = 0.5, Reaction temp = 80°C.**

### 5.3.4 Effect of ligands (BPMODA vs. EHA<sub>6</sub>-TREN)

Ligands are able to affect the ATRP equilibrium. In ATRP, the presence of an X-Cu<sup>II</sup> / ligand complex is necessary to reduce the concentration of radicals through a deactivation process to maintain the activation-deactivation equilibrium for the controlled growth of the polymer chains<sup>(46)</sup>. The catalyst activity increases with the increasing number of nitrogen coordination sites, N<sub>4</sub> > N<sub>3</sub> > N<sub>2</sub> >> N<sub>1</sub><sup>(47)</sup>. The EHA<sub>6</sub>-TREN having four nitrogen coordination sites is a very active ATRP ligand. For a specific ligand, the concentration of propagating radicals and the rate of deactivation need to be adjusted to maintain polymerization control. If too many radicals are generated during the initiation step, irreversible radical termination will reduce the initiator efficiency and slow down the polymerization. To obtain well-defined polymers with low polydispersities, it is crucial to rapidly deactivate the growing chains to form dormant species<sup>(48)</sup>.

**Table 5- 4 The effect of BPMODA vs. EHA<sub>6</sub>-TREN on BA polymerization**

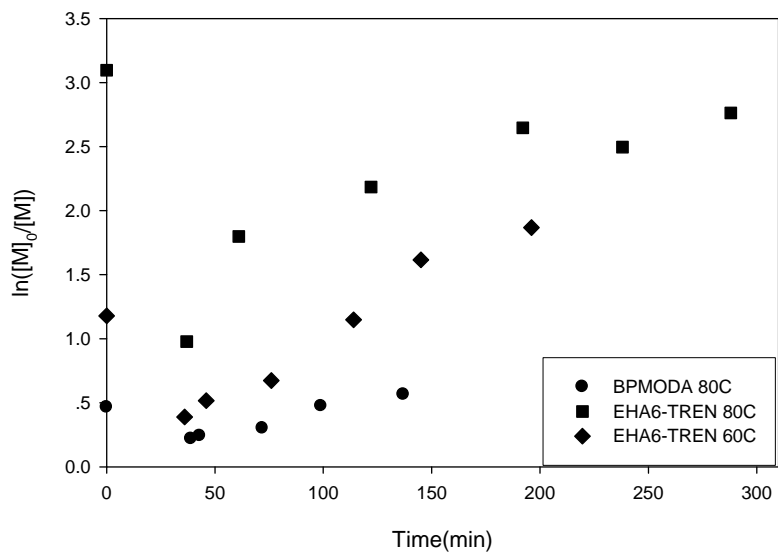
Ligand	Surfactant	Temp. °C	Time (min)	Conversion %	M <sub>n, GPC</sub> (g/mol)	M <sub>n, Cal</sub> (g/mol)	Mw/ Mn
BPMODA	Brij98	80	127	43.11	21698	15840	1.86
EHA <sub>6</sub> TREN		80	278	93.69	33422	35856	2.09
		60	135	80.14	40924	36150	1.82
BPMODA	CTAB	80	368	34.06	12632	9769	bimodal
EHA <sub>6</sub> TREN		60	158	69.92	50548	16894	3.04
		55	220	87.36	62587	21193	3.91

Brij98 or CTAB was used as surfactant, [CuBr<sub>2</sub>]/ [EBiB] = 0.5, [Brij98]/[BA] = 74 wt%, [CTAB]/[BA] = 36 wt%.

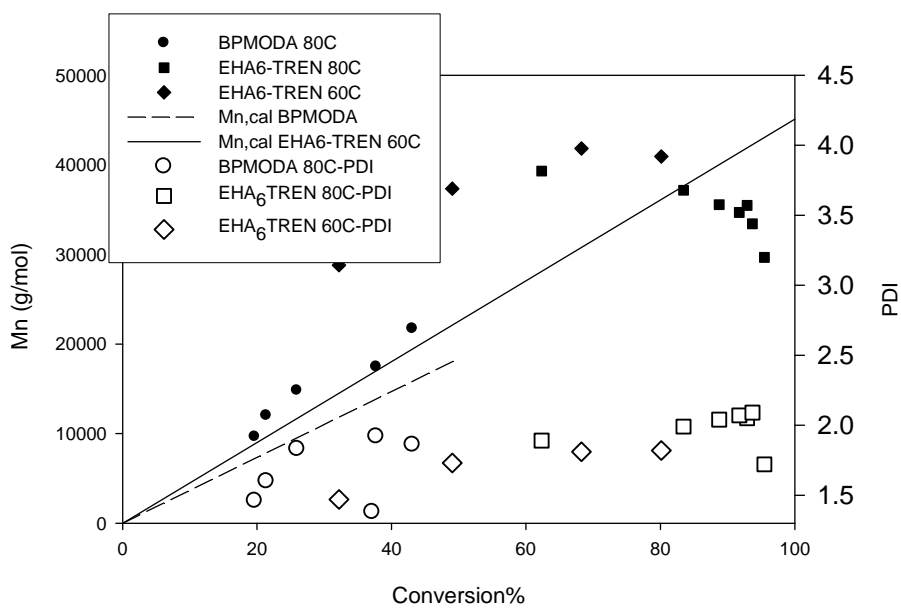
(Mn values, for bimodal peaks, measured for the growing molecular peaks.)

EHA<sub>6</sub>-TREN was used as a ligand in the AGET ATRP of BA microemulsion polymerization and compared with BPMODA. Brij98 and CTAB were used as surfactants. The experimental conditions and results are summarized in Table 5-4. When EHA<sub>6</sub>-TREN/CuBr<sub>2</sub> was used as a catalyst, fast and non-controlled polymerizations were observed from both surfactants Brij98 and CTAB (Table 5-4). In the first-order plots, when Brij98 was used as surfactant, faster polymerization rates were observed using CuBr<sub>2</sub>/EHA<sub>6</sub>-TREN as the catalyst, and relatively slower polymerization rates were seen using CuBr<sub>2</sub>/BPMODA as the catalyst (Figure 5-7 (a)). Molecular weights agreed fairly well with the theoretical values when CuBr<sub>2</sub>/BPMODA was used. There was greater deviation between experimental molecular weights and theoretical values when CuBr<sub>2</sub>/EHA<sub>6</sub>-TREN was used, indicating a poorly controlled system (Figure 5-7 (b)). At the same time, the polydispersity increased over the course of polymerization. Since activity of EHA<sub>6</sub>-TREN is high, fast polymerization was obtained. The initial molecular weights were higher than the expected values, indicating lower initiation efficiency and termination at the beginning, which is consistent with the high initial conversion when CuBr<sub>2</sub>/EHA<sub>6</sub>-TREN was used.

In the GPC traces (Figure 5-8), when the Brij98 was used as surfactant, the molecular weight grew just a little at the very beginning of the reaction, and then stopped, possibly due to fast termination.



(a)



(b)

**Figure 5- 7 Comparison of BPMODA and EHA<sub>6</sub>-TREN (a) first-order plots and (b) evolution of Mn versus conversion**

**[Brij98]/ [BA] = 74 wt%, [CuBr<sub>2</sub>]/ [EBiB] = 0.5, Reaction temp = 80°C and 60°C, respectively.**

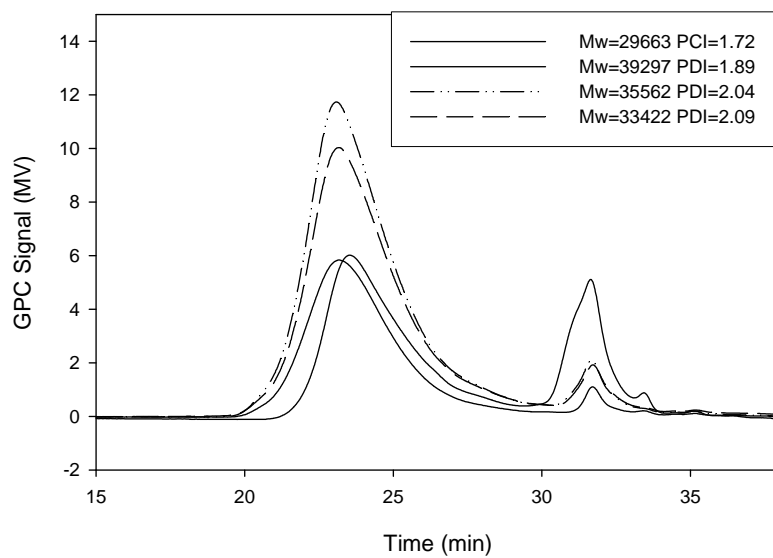
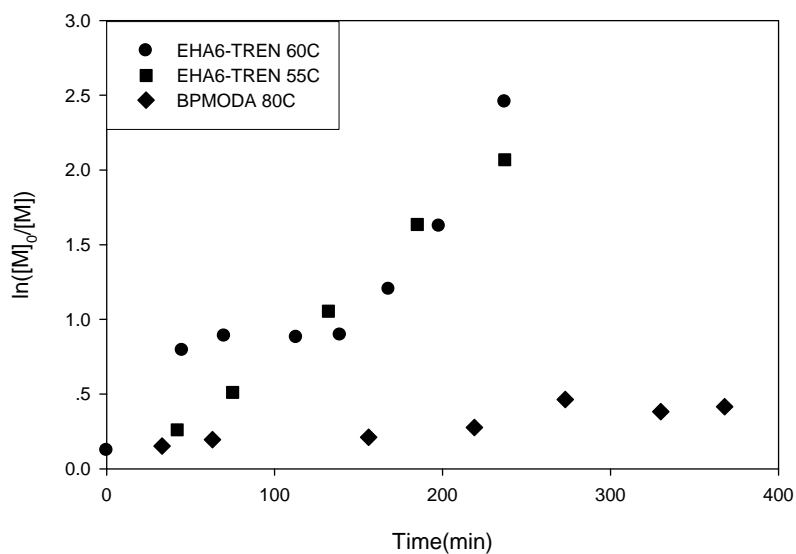
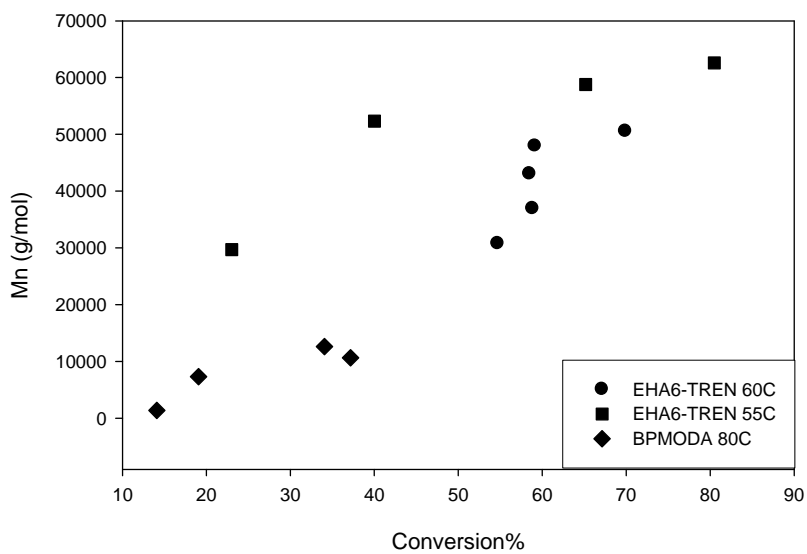


**Figure 5- 8 GPC traces of BA polymerization using  $\text{CuBr}_2/\text{EHA}_6\text{-TREN}$  as the catalyst  
 $[\text{Brij98}]/[\text{BA}] = 74 \text{ wt\%}$ ,  $[\text{CuBr}_2]/[\text{EBiB}] = 0.5$ , Reaction Temp =  $80^\circ\text{C}$ .**

From this study, when Brij98 was used as surfactant, a controlled polymerization was obtained using BPMODA as ligand. When  $\text{EHA}_6\text{-TREN}$  was used as ligand, fast polymerization was observed yielding non-controlled results.



(a)



(b)

**Figure 5- 9 Comparison of BPMODA and EHA<sub>6</sub>-TREN (a) first-order plots and (b) evolution of Mn versus conversion**

**[CTAB]/ [BA] = 36 wt%, [CuBr<sub>2</sub>]/ [EBiB] = 0.5, Reaction temp = 80°C and 60°C, respectively.**

When CTAB was used as surfactant, similar results were obtained as Brij98. Fast polymerization rates were observed in EHA<sub>6</sub>-TREN in the conversion profiles and slower rates were found in BPMODA (Figure 5-9 (a)). The molecular weight and theoretical values were in good agreement with BPMODA, but the deviations were quite high when EHA<sub>6</sub>-TREN was used, suggesting that the activity of EHA<sub>6</sub>-TREN is too high to control the polymerization (Figure 5-9(b)). When the experiment was conducted with CuBr<sub>2</sub>/BPMODA, there were bimodal peaks observed in GPC traces, similar to those discussed in the previous sections. There was no growth trend in molecular weight in the EHA<sub>6</sub>-TREN system, based on the GPC traces (Figure 5-10), indicating a poorly controlled polymerization.

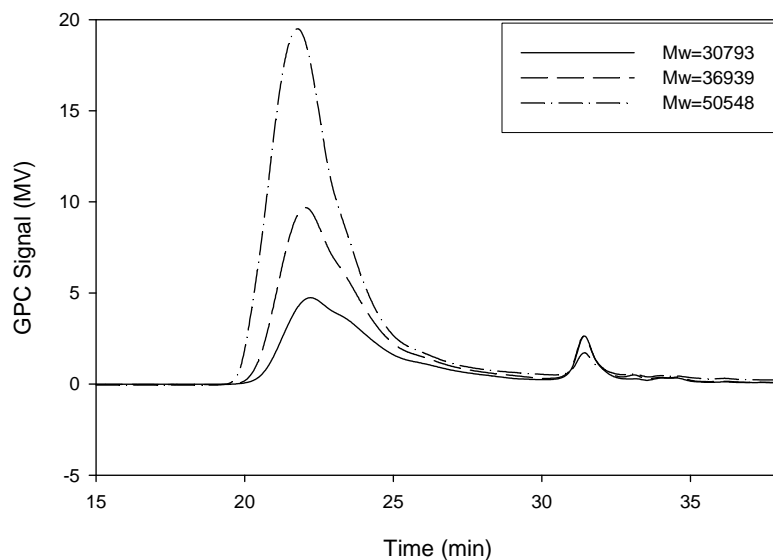


**Figure 5- 10 GPC traces of BA polymerization using CuBr<sub>2</sub>/EHA<sub>6</sub>-TREN as the catalyst  
[CTAB]/ [BA] = 36 wt%, [CuBr<sub>2</sub>]/ [EBiB] = 0.5, Reaction Temp =60°C.**

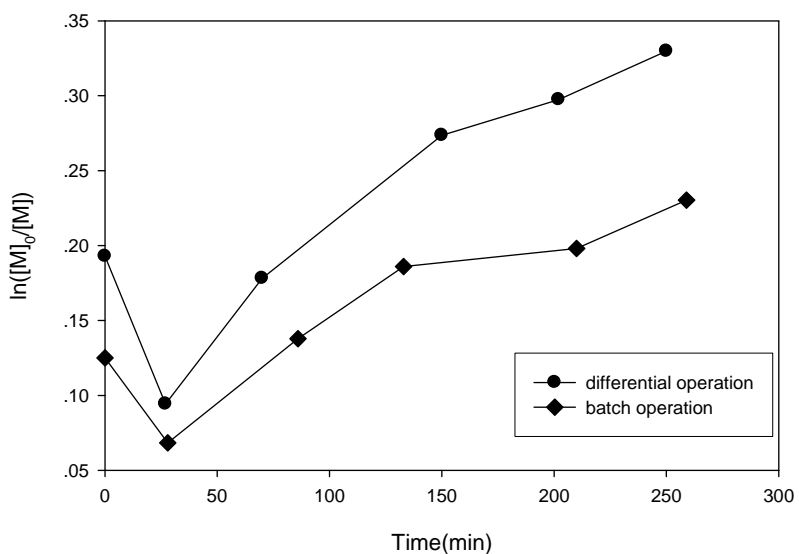
All the results indicated that  $\text{CuBr}_2/\text{BPMODA}$  is an appropriate catalyst for BA in AGET ATRP microemulsion polymerization. It yielded better controlled polymerization than using  $\text{EHA}_6\text{-TREN}$  as ligand.

### **5.3.5 Effect of monomer addition and temperature**

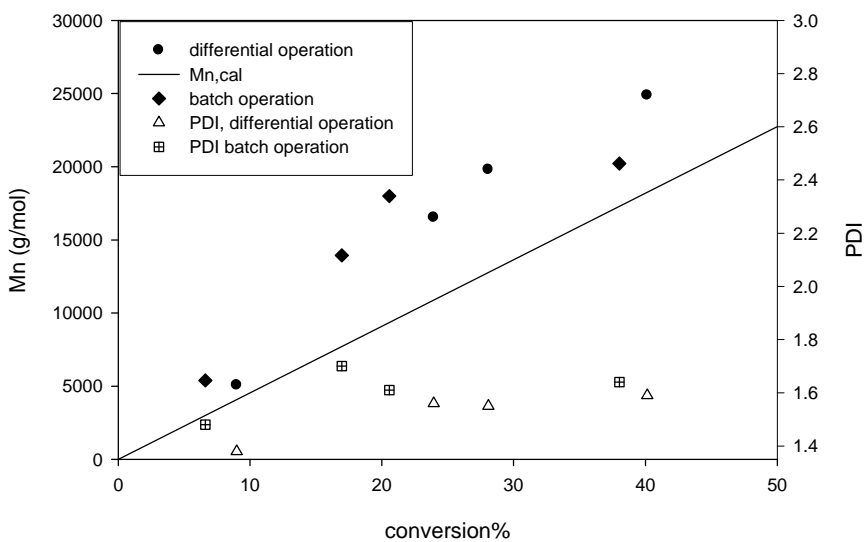
#### **Differential Method vs. Batch Method**

The differential microemulsion polymerization method is able to decrease the amount of surfactant required compared to conventional microemulsion polymerization. In this section, the differential method was compared with the traditional batch method for AGET ATRP.

Figure 5-11 (a) showed that the slower polymerization rate was obtained in the batch operation. In the differential operation, monomer was added at a very slow rate and was quickly consumed by the growing chains in the polymer particles. On the other hand, in batch polymerization, monomer droplets were formed as a reservoir and monomer molecules had to transfer from the organic phase into the aqueous phase first to reach the propagating polymer particles, leading to a slower polymerization rate. Since the CTAB was a very effective surfactant in forming the small particles, the particle size obtained in these two methods was similar (~10 nm).



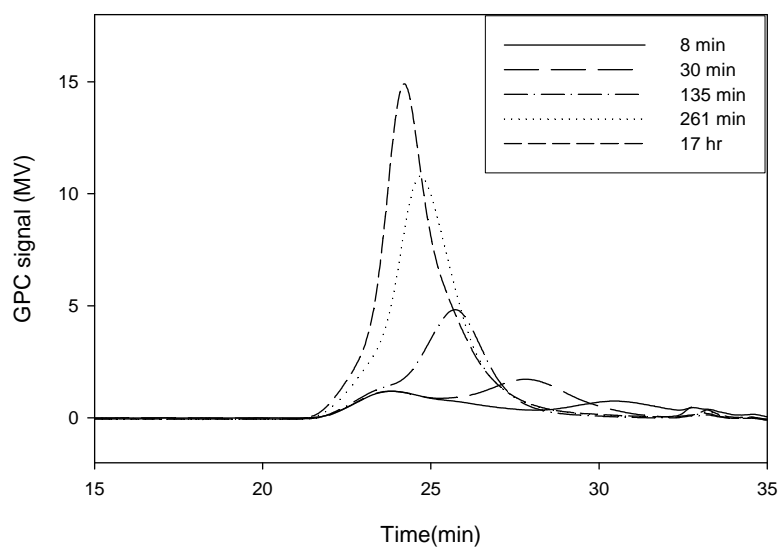
(a)



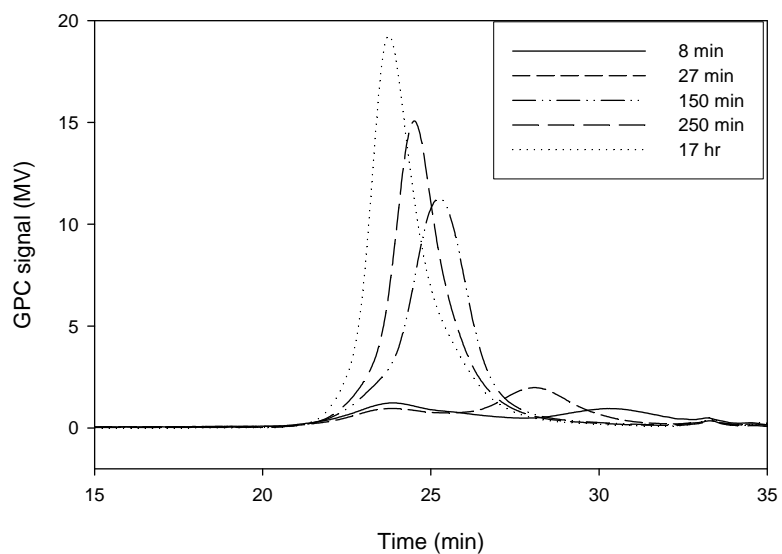
(b)

**Figure 5- 11 Comparison of differential method and batch method (a) first-order kinetic plots and (b) molecular weight dependence**

**[BA]: [EBiB]: [CuBr<sub>2</sub>]: [BPMODA]: [ascorbic acid] = 243:1:0.47:0.70:0.20, [CTAB]/ [BA] =35.6 wt%, Reaction temp = 80°C.**



(a)



(b)

**Figure 5- 12 Comparison of batch method (a) and differential method (b) on GPC traces**

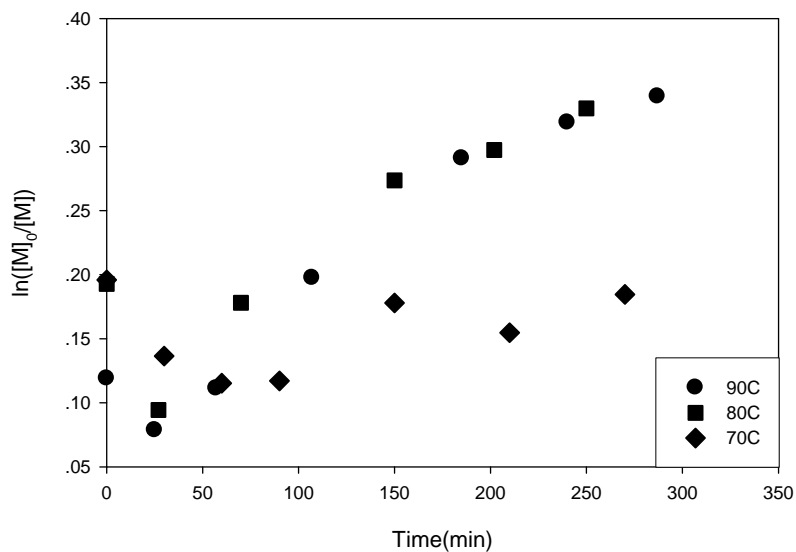
**[BA]: [EBiB]: [CuBr<sub>2</sub>]: [BPMODA]: [ascorbic acid] = 243:1:0.47:0.70:0.20, [CTAB]/ [BA] = 35.6 wt%, Reaction temp = 80°C.**

Molecular weights ( $M_n$ ) increased with conversion in both methods and experimental molecular weights were greater than theoretical values, suggesting inefficient initiation or possibly radical coupling termination. The polydispersities were about 1.5 in both methods, (Figure 5-11 (b)). In Figure 5-12, the GPC traces by both methods showed bimodal peaks at the beginning, and then only one broad peak was found over the course of polymerization. The GPC traces showed noticeable evolution of molecular weight in both methods, but the growth was more significant in the differential method.

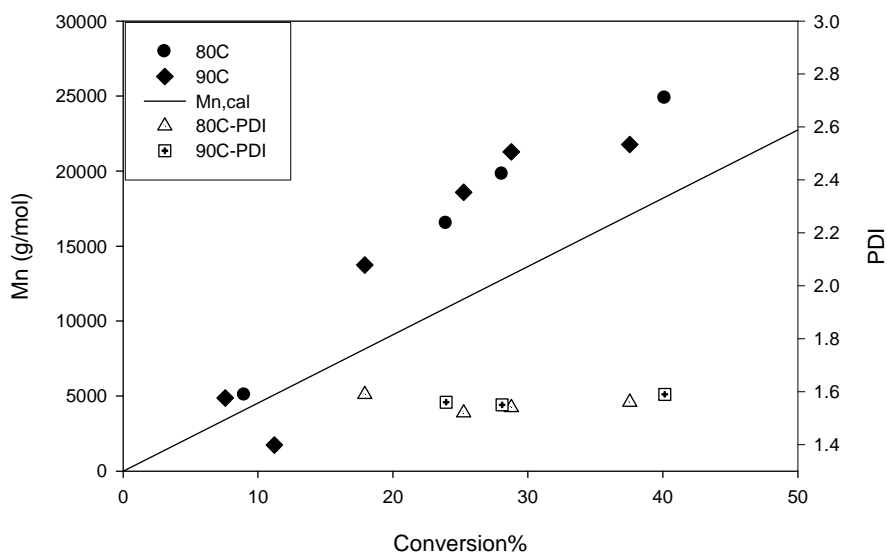
### **Effect of Temperature**

The rate of polymerization increases with increasing temperature due to both increasing propagating rate and atom transfer equilibrium constant, according to the equation of ATRP polymerization rate <sup>(9)</sup>. BA was normally polymerized at 80°C, but the polymerization was also performed at 70°C and 90°C as a comparison.

The first-order kinetic plots of the polymerizations are shown in Figure 5-13 (a). There was an increase in the rate of polymerization at higher temperature as expected. However, lower initial conversion was obtained at 90°C and higher initial conversion was obtained at 80°C, but there was no significant difference between these two temperatures after the initial polymerization. When the molecular weight data were analyzed (Figure 5-13 (b)), the number-average molecular weight values were greater than predicted values, but polydispersities were fairly narrow ( $M_w/M_n \sim 1.5$ ). There was no significant difference between the two reactions at 80°C and 90°C in terms of molecular weight control. However, the GPC traces of the reaction at 90°C showed a poor control trend comparing to the GPC traces at 80°C. This may be due to faster polymerization resulting in termination reactions.



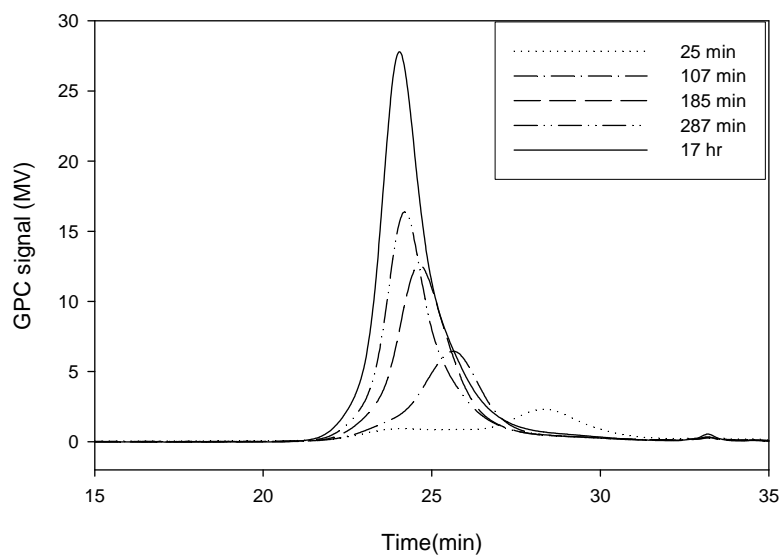
(a)



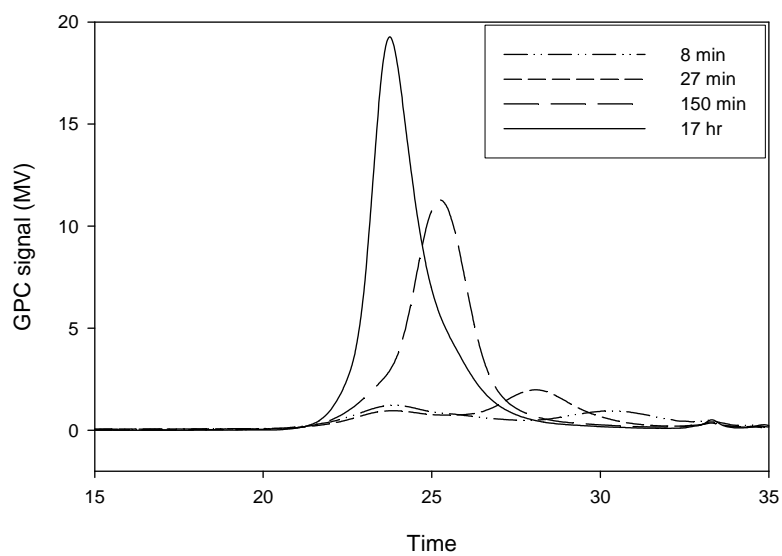
(b)

**Figure 5- 13 The effect of temperature on BA polymerization (a) First-order kinetic plots and (b) evolution of Mn and Mw/Mn versus conversion**

**[BA]: [EBiB]: [CuBr<sub>2</sub>]: [BPMODA]: [ascorbic acid] =354:1:1.22:1.77:0.44, [CTAB] = 27.6 wt% vs. monomer.**



(a)



(b)

**Figure 5- 14 GPC traces of the effect of temperature on BA polymerization (a) 90°C and (b) 80°C**

**[BA]: [EBiB]: [CuBr<sub>2</sub>]: [BPMODA]: [ascorbic acid] = 354:1:1.22:1.77:0.44, [CTAB] = 27.6 wt% vs. monomer.**

## 5.4 Conclusion

AGET ATRP has been successfully applied to a microemulsion polymerization using a “two-step” procedure, in which the microemulsion was formed by continuously feeding the monomer into a preformed microemulsion system. When CTAB was used as surfactant in the polymerization, small sized particles (<20 nm) were formed, and the molecular weight was controlled, with the polydispersity of about 1.5. Bimodal peaks showed up in GPC traces, but it was not significant when the concentration of catalyst was high. Particle sizes of the final latexes were increased by decreasing the concentration of surfactant and well-controlled polymerization was observed with less surfactant. Comparing the use of CTAB and Brij98, CTAB was preferable in forming small sized particles in a controlled polymerization. Additionally, the differential method gave a slightly better controlled polymerization than the traditional batch method. Comparing with BPMODA, EHA<sub>6</sub>-TREN had a rapid polymerization rate and poor control.

## Chapter 6

### AGET ATRP of Butyl Methacrylate

#### 6.1 Introduction

The concept of microemulsion polymerization appeared around 1980. Microemulsion has many interesting features, such as large internal interfacial area, optical transparency, thermodynamic stability, and great variety of structures <sup>(49)</sup>. However, conventional microemulsion yields high molecular weight polymers and broad polydispersities. Living/controlled radical polymerization (L/CRP) techniques provides a facile route to synthesizing polymers with predetermined molecular weight and narrow polydispersities. Atom transfer radical polymerization (ATRP) is one of the L/CRP techniques, but only one study has applied ATRP in microemulsion. In Min's study, better results were obtained from AGET ATRP than from either normal ATRP or reverse ATRP in microemulsion when methyl methacrylate (MMA) was used as monomer, polyoxyethylene(20) oleyl ether (Brij98) as surfactant, and Bis (2-pyridylmethyl) octadecylamine (BPMODA) as ligand <sup>(22)</sup>. The average diameter particle size was 43 nm and polydispersity was 1.28. However, the weight ratio of surfactant to monomer was very high ( $[\text{surfactant}]/[\text{MMA}] \sim 2.5$ ), which is a common problem in microemulsion. In our group's studies, butyl acrylate (BA) was investigated in AGET ATRP microemulsion polymerization using a differential method. The cationic surfactant cetyltrimethylammonium bromide (CTAB) and BPMODA ligand were used in the system, and small sized particles (<20 nm) were formed, yielding controlled molecular weight polymer with polydispersity about 1.5.

A variety of monomers have been successfully polymerized using ATRP <sup>(50)</sup>. Each monomer has its own unique atom transfer equilibrium constant even when the other polymerization conditions are kept as the same. The copper-mediated ATRP of methacrylates displays a significantly higher equilibrium constant when compared with acrylates <sup>(43)</sup>. BA and BMA (butyl methacrylate) have

different physical parameters (e.g. BMA is less soluble in water) as well as kinetic parameters. In this work, BMA was used as a monomer in AGET ATRP microemulsion polymerization to assess the suitability of the microemulsion ATRP process for BMA.

## **6.2 Experimental**

### **Materials**

n-Butyl methacrylate (BMA, Aldrich) was purified by passing through a column packed with inhibitor remover (Aldrich). The compounds copper (II) bromide ( $\text{CuBr}_2$ , 99 % Aldrich), cetyltrimethylammonium bromide (CTAB, 95 % Aldrich), polyoxyethylene (20) oleyl ether (Brij98, Aldrich), ethyl 2-Bromoisobutyrate (EBiB, 98 % Aldrich), L-Ascorbic Acid ( $\text{C}_6\text{H}_8\text{O}_6$ , 99 %, Sigma) were used as received. The synthesis of BPMODA was adapted from a literature method<sup>(35)</sup>.

### **Microemulsion polymerization**

The organic phase was prepared by dissolving copper (II) bromide ( $\text{CuBr}_2$ , 0.0331 g, 0.148 mmol) and BPMODA (0.1102 g, 0.244 mmol) in BMA (5 ml) in a beaker and stirring overnight at room temperature to form a homogeneous solution. The initiator, ethyl 2-bromoisobutyrate (EBiB, 0.0732 g, 0.375 mmol), was then dissolved in this mixture. After stirring for 30 min, a one-fifth fraction of the mixture (0.9349 g) was taken out as the organic phase. The aqueous phase consisting of the surfactant cetyltrimethylammonium bromide (CTAB, 36 wt % vs. monomer) and deionized water (DIW, 30 mL) was stirred for 30 min before the organic phase was added. An initial microemulsion was formed by stirring for 60 min under nitrogen. The initial microemulsion was then immersed in an oil bath that was preheated to 80° C. The reducing agent solution (0.5 ml) containing L-ascorbic acid (1.73 mg) was purged with nitrogen for 20 min

and injected into the initial microemulsion with a deoxygenated syringe to initiate the polymerization. After polymerizing for five minutes, the predeoxygenated second part of BMA (2 mL) was added drop-wise to the microemulsion over 20 min, and typically 4 more hours were required for completion of the polymerization. Samples were taken at regular intervals and placed into an ice bath before analysis.

### **Characterization**

Monomer conversions were determined gravimetrically. Gel permeation chromatography (GPC) was used to measure the molecular weight and polydispersity of the polymer samples. Dried polymer samples were dissolved in tetrahydrofuran (THF) and passed through a column packed with aluminum oxide to remove the residual copper. The GPC was performed using a Waters 2960 Separation Module with four Styragel columns of pore sizes 100, 500,  $10^3$  and  $10^4$  Å. Flow rate of the eluant, THF, was set at 1.0 mL/min. Polystyrene standards were used for calibration. The Zeta-Sizer Nano-ZS (Malvern) was used to measure particle sizes using Dynamic Light Scattering (DLS). Samples were diluted before measuring.

## **6.3 Results and Discussion**

### **Effect of Temperature**

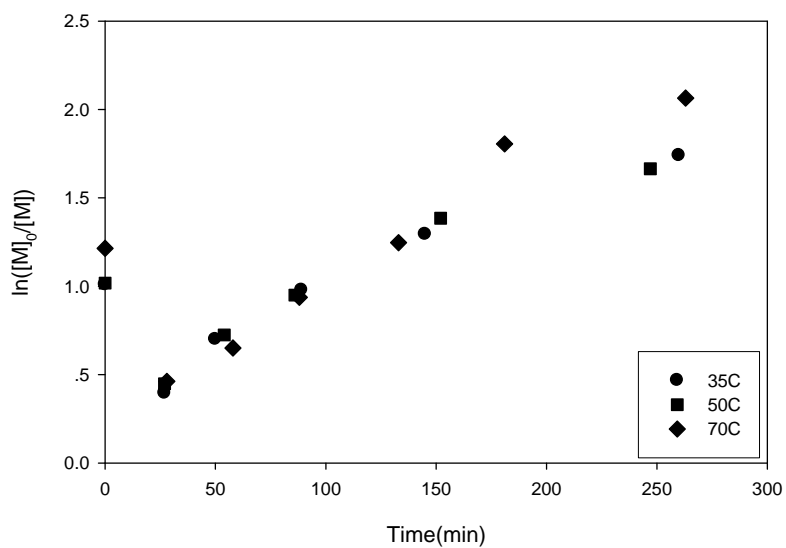
Temperature is a key factor affecting propagation rate and the ATRP equilibrium constant. The effect of temperature was investigated at three different temperature; 35°C, 50°C, and 70°C, respectively (Table 6-1).

**Table 6- 1 Effect of Temperature on BMA polymerization**

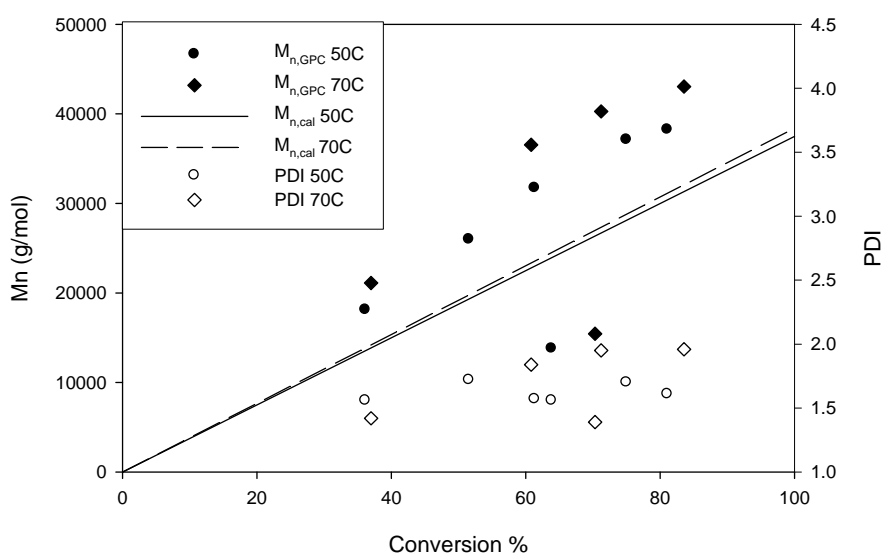
Temperature °C	Time (min)	Conversion %	$M_{n, GPC}$ (g/mol)	$M_{n, Cal}$ (g/mol)	Mw/Mn
35	260	82.45	32215	30997	1.6
50	247	81.07	38241	30391	1.61
70	263	87.31	43042	32069	1.96

[CuBr<sub>2</sub>]/ [EBiB] = 0.5, [CTAB]/ [BMA] = 36 wt %.

In all experiments, conversion reached over 80 % in about 4 hr, but the polydispersities were relatively high. The first-order plots indicated high initial conversion in BMA microemulsion polymerization at all three temperatures. Relatively higher initial conversion was obtained at the high temperature (70°C). After the initial point, the conversion profile was similar for the three temperatures (Figure 6-1 (a)). From the evolution of molecular weight (Figure 6-1 (b)), the initial number of chains was more than that at the end of the experiment implying the existence of termination. The experimental Mn values were greater than the theoretical values for both the experiments at 50°C and 70°C, with the smaller deviation at 50°C. The molecular weight distribution was narrow at 50°C as well. For the experiment run at 70°C, the polydispersity increased over the course of polymerization and reached to about 2.0 in the end.



(a)



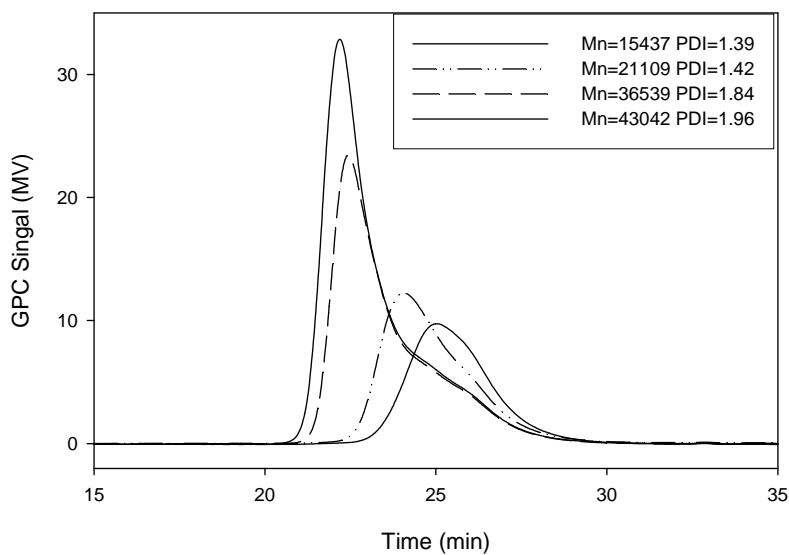
(b)

**Figure 6- 1 The effect of Temperature on BMA polymerization (a) first-order plots and (b) Mn vs. Conversion of BMA**

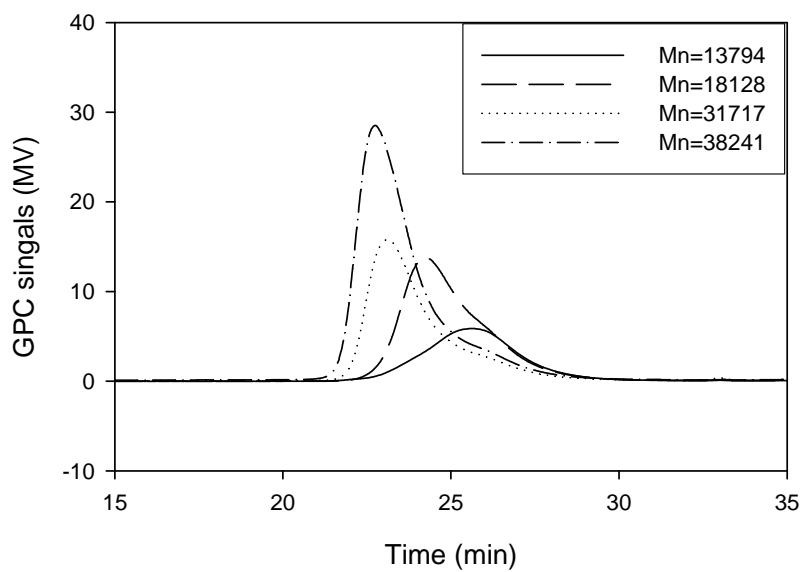
**[CuBr<sub>2</sub>]/ [EBiB] = 0.5, [CTAB]/ [BMA] = 36 wt %.**

In the GPC traces, a low-molecular-weight tail was observed resulting in broad polydispersity. A possible reason for the tailing is that the polymerization was very fast in BMA and many active chains were formed at the beginning of the polymerization leading to radical termination and the formation of low-molecular-weight dead chains. At 35°C, bimodal peaks were observed initially in the GPC traces, probably because at the low temperature the ATRP equilibrium constant was too low resulting in a slow establishing of the ATRP equilibrium. Subsequently, no significant growing trend was shown in the GPC traces indicating a poorly controlled polymerization at 35°C.

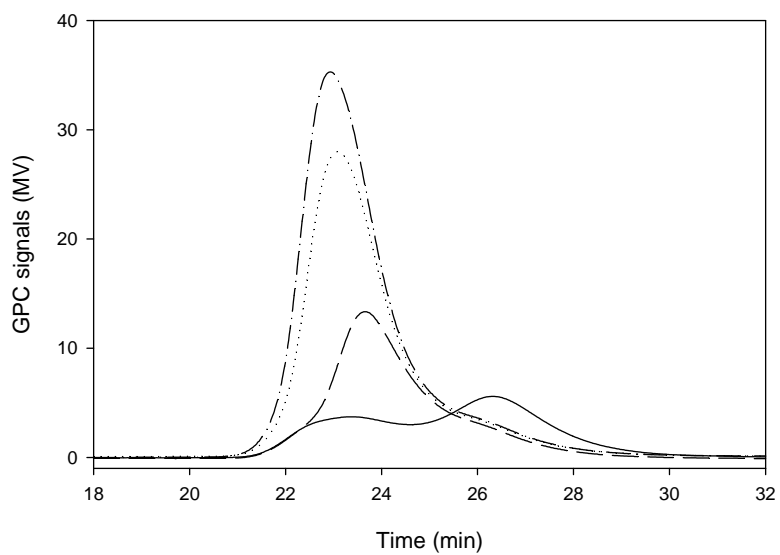
Overall, decreasing temperature can improve the livingness of polymerization, but too low a temperature, such as 35°C, also leads to a poorly controlled system.



(a)



(b)



(c)

**Figure 6- 2 GPC traces of BMA polymerization at different temperature (a) 70°C, (b) 50°C, and (c) 35°C**

**[BMA]: [EBiB]: [CuBr<sub>2</sub>]: [BPMODA]: [ascorbic acid] = 270:1:0.51:0.74:0.21, [CTAB]/ [BMA] =36 wt%.**

### **Effect of the concentration of the reducing agent**

Ascorbic acid was selected as the reducing agent in this work, because it is a strong reducing agent and can quickly convert Cu(II) to Cu(I). AGET ATRP can tolerate a relatively large range of concentration of reducing agent <sup>(21)</sup>. The appropriate amount of reducing agent is crucial to achieve a controlled polymerization. Too small amount of ascorbic acid would lead to a very slow polymerization, whereas too large amount would lead to a reduced level of control. In miniemulsion polymerization the best ratio of [Cu(II)]/[ascorbic acid] is 2.5 <sup>(20)</sup>. Three ratios of [Cu(II)]/[ascorbic acid] (1.97, 2.5, and 3.01) were investigated in this study (note that ascorbic acid is a two-electron reducing agent).

High initial conversion was observed in all three reactions. After the initial point, a slow polymerization rate was observed with the ratio of [CuBr<sub>2</sub>]/[ascorbic acid] of 2.5 (Figure 6-3 (a)). The conversion profile showed faster polymerization rates with the other two ratios, 3.01 and 1.97, but no significant differences were observed between those two ratios. Molecular weight increased with conversion for these three reactions. With the ratio of 2.5, experimental molecular weight agreed fairly well with predicted values. With the other two ratios, the experimental molecular weights were larger than theoretical values, but the Mn profiles were similar (Figure 6-3 (b)). Polydispersity was fairly low (~1.5), with the ratio of 2.5. In the other two experiments, polydispersities were higher, and the polydispersities increased with polymerization time indicating the presence of termination.

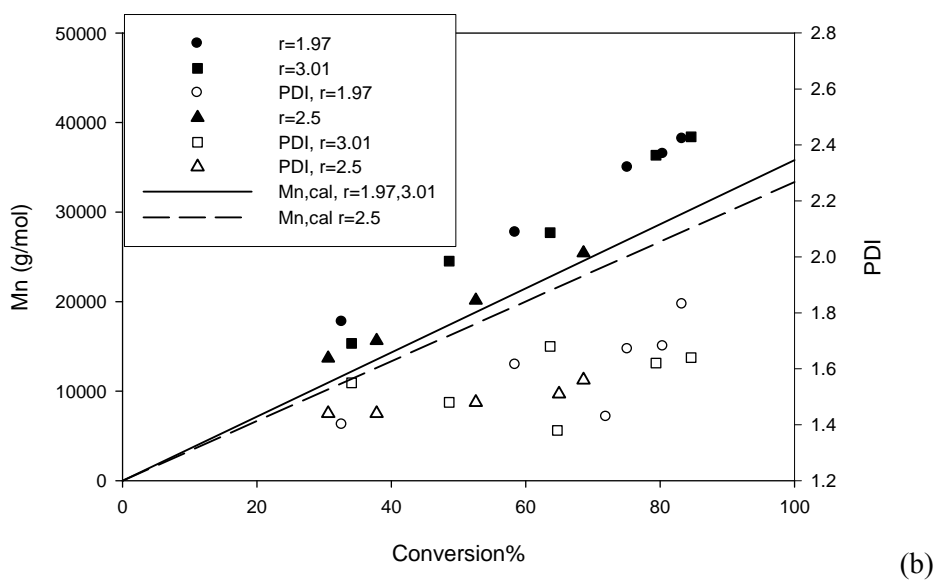
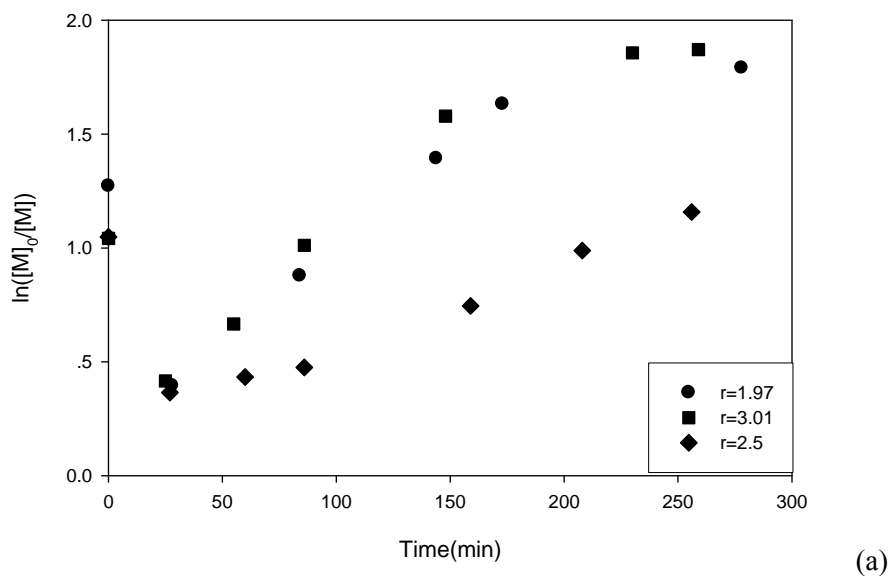


**Figure 6- 3 The effect of ascorbic acid concentration on BMA polymerization (a) first-order plots and (b) molecular weight and Mw/Mn versus conversion**

[Cu(II)]/[ascorbic acid] = 1.97, 2.5 and 3.01, respectively. [CuBr<sub>2</sub>]/ [EBiB] = 0.4, [CTAB]/ [BMA] = 30 wt%, Reaction temp = 70°C

The Mn-conversion profile showed a better controlled trend at the ratio of 2.5, as evidenced by better agreement between experimental molecular weights and theoretical values, and fairly low polydispersity. The polymerization conducted at an [Cu(II)]/[ascorbic acid] ratio of 2.5 indicated a better controlled polymerization compared to the other ratios used.

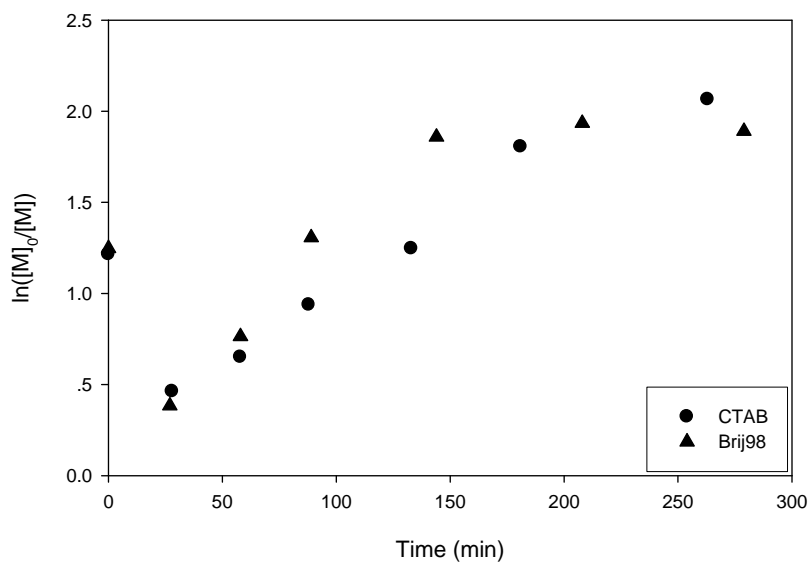
#### Effect of different surfactants (CTAB vs. Brij98)

Surfactant is very important in stabilizing the microemulsion system, and different surfactants might have different effects on the polymerization. To find the most suitable surfactant in the microemulsion polymerization of BMA, the cationic surfactant CTAB and the nonionic surfactant Brij98 were studied. The results are summarized in Table 6-2. Both experiments reached over 80% conversion in about three hours, but both of the polydispersities were quite high.

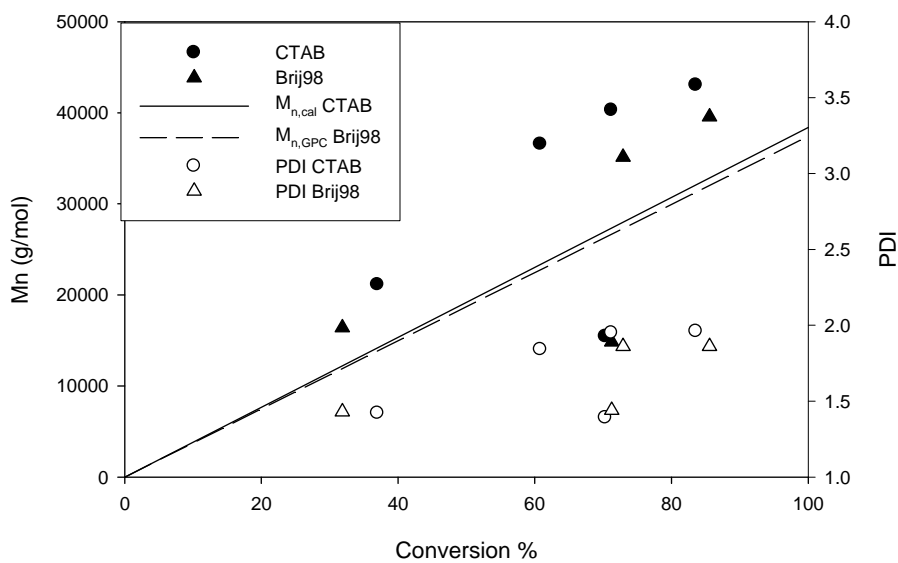
**Table 6- 2 The effect of Brij98 on BMA polymerization**

	Surfactant	[surfactant]:[BA]=R wt%	Time (min)	conversion %	M <sub>n,GPC</sub> (g/mol)	M <sub>n,Cal</sub> (g/mol)	PDI
BMA	Brij98	36	198	85.55	39556	32016	1.86
	CTAB	36.9	171	83.55	43042	32069	1.96

[CuBr<sub>2</sub>]/ [EBiB] = 0.5, Reaction temp = 70°C.



(a)



(b)

**Figure 6- 4 The effect of surfactants on BMA polymerization (a) Conversion evolution and (b) molecular weight dependence**

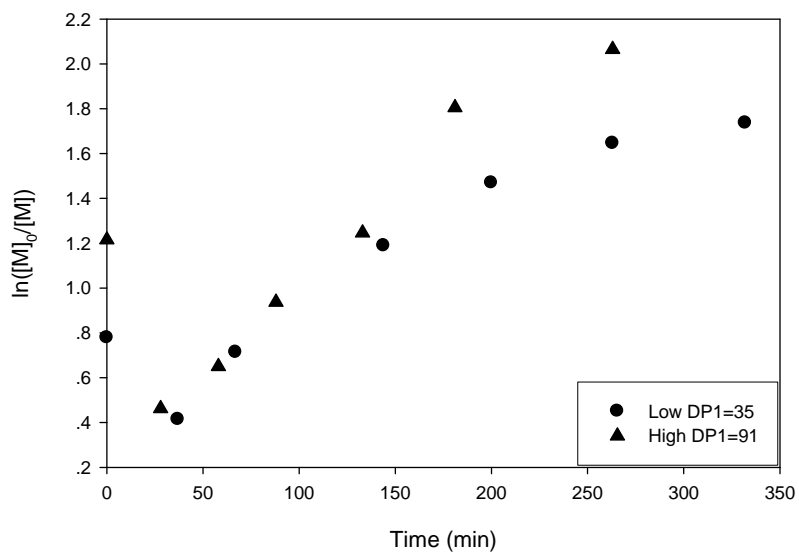
[surfactant] vs. [BMA] ~36 wt %. [CuBr<sub>2</sub>]/ [EBiB] = 0.5, Reaction temp = 70 °C.

In the first-order plots, high initial conversion was obtained in both CTAB and Brij98, and the initial conversion was almost the same in the two experiments. After the beginning, Brij98 showed a little faster polymerization rate than CTAB, but noticeable curvature showed in the conversion plots, indicating decreasing concentration of propagating radicals (Figure 6-4 (a)). For both experiments, the initial number of chains was higher than at the end of the experiments implying the existence of termination (Figure 6-4 (b)). Experimental molecular weight was greater than theoretical values in both experiments, and the polydispersities were both quite high. CTAB showed even greater deviation between experimental molecular weights and theoretical values, suggesting the presence of radical termination. By DLS measurement, the particle size was 4.8 nm (0.48 (No. Cu / per particle)) in Brij98, and the particles size nm was 8.5 nm in CTAB (2.2 (No. Cu / per particle)). These values are probably unrealistically low but they do indicate very small particles were made.

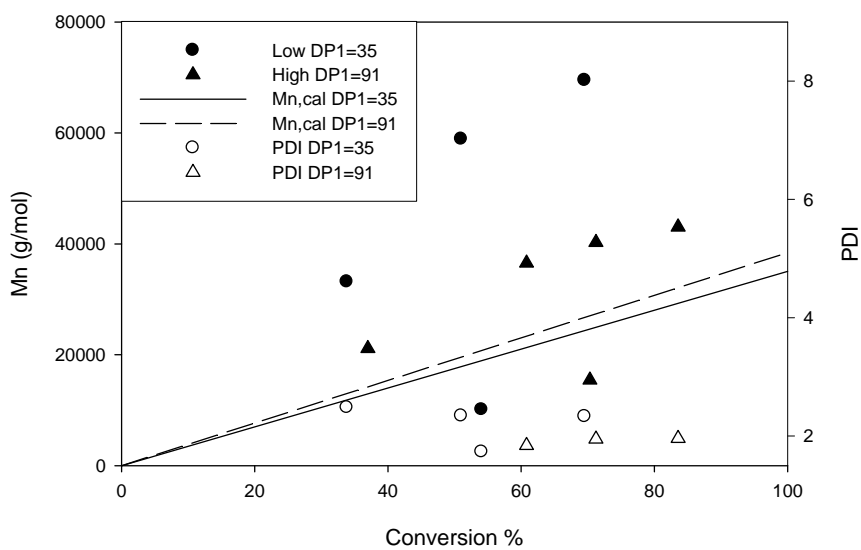
#### **Effect of the degree of polymerization (DP) at the first stage**

A two step polymerization procedure was used in this study. Since all the catalyst, surfactant and ligand were added in the first step, it is very crucial for the performance of the polymerization. Theoretically, reducing the DP achieved in the first step might influence the required surfactant concentration and catalyst concentration. In this work, different initial DPs were investigated to get a well controlled polymerization. The results for a low DP (35) and a high DP (90) are shown below.

A lower initial conversion was obtained with lower  $DP_1$  as expected, but curvature was observed at the end of the experiment indicating the presence of radical termination (Figure 6-5 (a)). In the evolution of molecular weight, very high molecular weights were obtained with lower  $DP_1$  (Figure 6-5 (b)). Both of the experiments showed quite high polydispersities.



(a)



(b)

**Figure 6- 5 The effect of degree of polymerization at the first stage on BMA polymerization  
(a) Conversion evolution and (b) molecular weight dependence**

**[CTAB]/ [BMA] = 36 wt %. [CuBr<sub>2</sub>]/ [EBiB] = 0.5, Reaction temp = 70°C.**

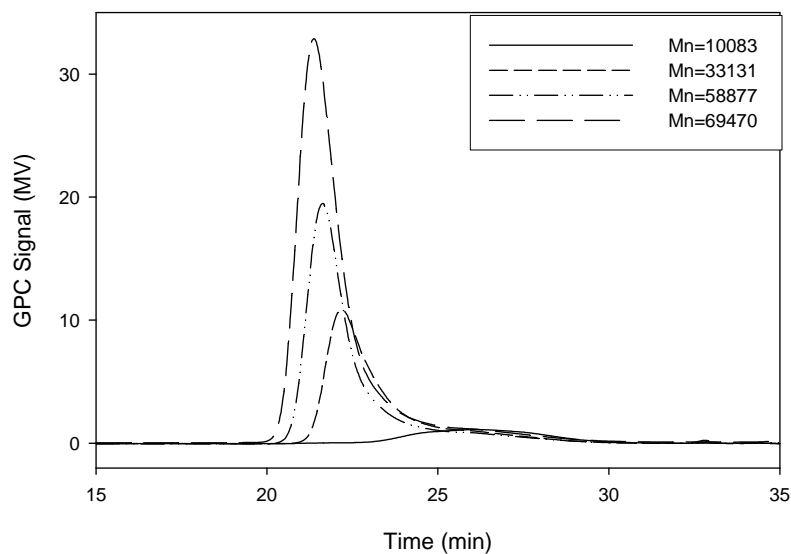


**Figure 6- 6 GPC traces at various DP<sub>1</sub> in BMA polymerization**

**DP<sub>1</sub> = 35, [CuBr<sub>2</sub>]/ [EBiB] = 0.5, [CTAB]/ [BMA] = 36 wt%**

The experiment with lower DP<sub>1</sub> showed a poorly controlled trend in the GPC traces (Figure 6-6). A long tail was seen, indicating radical termination at the beginning, and no remarkable growth after that point.

## 6.4 Conclusion

BMA polymerization showed very fast reaction rate, and the initial conversion reached very high values in a short time, resulting in a small-low-molecular weight tail in the GPC traces. Consequently, poorly controlled polymerizations were obtained. Decreasing temperature improved the livingness of polymerization, but too low temperature also led to less controlled polymerization. A better controlled polymerization was obtained with a ratio of copper and

reducing agent equal to 2.5. Reducing the degree of polymerization at the first step decreased the initial conversion, but poorly controlled polymerization was also observed.

## Chapter 7

### Conclusions

In this study, small sized nanoparticles (~40 nm) with controlled molecular distribution (polydispersity ~1.5) were successfully synthesized using a differential microemulsion process at a low surfactant concentration (surfactant/monomer ~ 1:3.5) in an aqueous system. AGET ATRP in a continuous two-step procedure is the most promising method to produce nanoparticles, while applying reverse ATRP was not successful in controlling molecular weight distribution, probably because of mass transfer problems. The cationic surfactant CTAB proved feasible in producing nanoparticles.

The effects of catalyst concentration, surfactants, ligands, temperature, and reducing agent concentration on polymerization were investigated. With increasing concentration of catalyst, the initial conversion was decreased in the first step, but the overall difference in conversion was not significant after addition of monomers in the second step. The effect of two different surfactants, CTAB and Brij98, on polymerization was similar and controlled polymerization was obtained for both of them. When the concentration of CTAB was decreased, slow polymerization rate and better control were observed. Two ligands, BPMODA and EHA<sub>6</sub>-TREN were compared, and only BPMODA proved to be readily applicable. The polymerization was too fast and not controlled when EHA<sub>6</sub>-TREN as used. Better controlled polymerization was obtained when the reaction temperature was 80 °C and the ratio of ascorbic acid and monomer is 2.5.

## Chapter 8

### Recommendations for Future Work

Although the two-step microemulsion process was shown to be a promising method in producing nanoparticles with low concentration of surfactant, and the effects of several factors on polymerization were investigated, this study should be looked upon as an initial step of a new polymerization technique. More detailed studies should be done before it can be applied as a general method at industrial scale. Several methods tested in this study showing the potential of controlled polymerization should be further studied and several problems need be solved.

1. The effect of catalyst concentration, surfactants, ligands, temperature, and reducing agent concentration on polymerization was only investigated one at a time, and not all the factors were simultaneously studied for a given monomer. Factorial design should be used to investigate the effect of multiple factors on the polymerization and find the most significant effects to optimize the system performance.
2. The polymerization system used in this study is quite complex. It is difficult to have a reasonable explanation for the experimental results if it is looked at a black box. A mechanistic model including the mass transfer between aqueous and oil phases, equilibrium kinetics of radical and dormant species, and the polymerization should be built to help understand the system behavior and solve more general problems.
3. Acetone was shown to help transport the catalyst into particles in several experiments. Optimization of experimental conditions, such as temperature, may allow for better control of the polymerization using this approach.
4. Bimodal peaks were generated in AGET ATRP microemulsion when BA was used as the monomer, showing that the polymerization was not controlled in the initial stages of

polymerization. It is important to understand the mechanism of the generation of the bimodal peak and find a solution for it.

5. The effect of surfactant on colloidal stability should be explored. This information will help understand the different results between ionic and non-ionic surfactants.

## References

1. He, G., Pan; Q. *Macromol Rapid Commun* 2004, 25, 1545-1548.
2. He, G.; Pan, Q.; Rempel, G.L. *Macromol Rapid Commun* 2003, 24, 585-588.
3. Min, K.; Gao, H.; Matyjaszewski, K. *J Am Chem Soc* 2006, 128, 10521-10526.
4. Georges, M. K.; Veregin, R. P. N.; Kazmaier, P. M.; Hamer, G. K. *Macromolecules* 1993, 26, 2987-2988.
5. Cunningham, M. F. *Prog. Polym. Sci.* 2002, 27, 1039-1067.
6. Asua, J. M. *Prog. Polym. Sci.* 2002, 27, 1283-1346.
7. Queffelec, J.; Baynor, S.G.; Matyjaszewski, L. *Macromolecules* 2000, 33(23), 8629-8639.
8. Tang, W.; Tsarevsky, NV; Matyjaszewski, K. *J Am Chem Soc* 2006, 128(5), 1598-1604.
9. Braunecker, WA.; Matyjaszewski, K. *Prog. Polym. Sci.* 2007; 32(1), 93-146.
10. Matyjaszewski, K.; Paik, H.; Zhou, P.; Diamanti, S.J. *Macromolecules* 2001, 34(15), 5125-5131.
11. Pintauer, T; Zhou, P; Matyjaszewski, K. *J Am Chem Soc* 2002, 124(28), 8196-8197.
12. Fischer, H. *J Polym sci Part A: Polym Chem* 1999, 37, 1885-1901.
13. Xia, J.; Matyjaszewski, K. *Macromolecules* 1999, 32(16), 5199-5202.
14. Li, M.; Matyjaszewski, L. *Macromolecules* 2003, 36(16), 6028-6035.
15. Simms, R. W.; Cunningham, M. F. *J Polym Sci A Polym Chem* 2006 44, 1628-1634.
16. Simms, R. W.; Cunningham, M. F. *Macromolecules* 2007, 40, 860-866.
17. Gromada, J; Matyjaszewski, K. *Macromolecules* 2001, 34(22), 7664-7671.

18. Jakubowski, W.; Matyjaszewski, K. *Macromolecules* 2005, 38(10), 4139-4146.
19. Braunecher, W.A.; Matyjaszewski, K. *prog. Polym. Sci.* 2007, 32(1), 93-146.
20. Min, K.; Gao, H.; Matyjaszewski, K. *J Am Chem Soc* 2005, 127, 3825-3830.
21. Min, K.; Jakubowski, W.; Matyjaszewski, K. *Macromol Rapid Commun* 2006, 27, 594-598.
22. Min, K.; Matyjaszewski, K. *Macromolecules* 2005, 38(20), 8131-8134.
23. Goddeeris, C.; Cuppo, F.; Reynaers, H.; Bouwman, W.G.; Van den Mooter, G. *International Journal of Pharmaceutics* 2006, 312(1-2), 187-195.
24. Min, K.; Gao, H.; Matyjaszewski, K. *Macromolecules* 2007, 40(6), 1789-1791.
25. Xu, X.; Gan, L. *Current opinion in colloid interface science.* 2005, 10(5-6), 239-244.
26. Rabelero, M.; Zacarias, M.; Mendizabal, E.; Puig, JE.; katime, I. *Polym Bull* 1997, 38, 695-700.
27. Gan, LM.; Lian, N.; Chew, CH.; Li, GZ. *Langmuir* 1994, 10(7), 2197-2204.
28. Dan, Y.; Yang, YH.; Chen, SY. *J Appl Polym Sci* 2002, 85, 2839-2844.
29. Ming, W.; Jones, FN.; Fu, SK. *Polym Bull* 1998, 40, 749-756.
30. Ming, W.; Jones, FN.; Fu, SK. *Macromol Chem Phys* 1998, 199, 1075-1079.
31. Hermanson, KD.; Kaler, EW. *Macromolecules* 2003, 36(6), 1836-1842.
32. Qian, R.; Wu, L.; Shen, D. *Macromolecules* 1993, 26(11), 2950-2953.
33. Pilcher, S.C.; Ford, W. T. *Macromolecules*, 1998, 31(11), 3454-3460.
34. He, GW. Thesis, 2006
35. Menger, F.M.; Lee, J. *J. Org. Chem.* 1993, 58(7), 1909-1916.

36. Klee, J.E.; Neidhart, F.; Flammersheim, H.J.; Mülhaupt, R. *Macromolecular Chemistry and Physics* 1999, 200, 517-523.
37. Zeng, F.; Shen, Y.; Zhu, S.; Pelton, R. *Macromolecules* 2000, 33, 1628-1635.
38. Qiu, J.; Charleux, B.; Matyjaszewski, K. *Prog. Polym. Sci.* 2001, 26, 2083-2134.
39. Chern, C.S.; Chen, T.J.; Wu, S.; Chu, H.B.; Huang, C.F. *J Macromol Sci Pure Appl Chem* 1997, 34, 1221.
40. Sajjadi, S. *J Polym Sci Part A* 2000, 38, 3612-3630.
41. Prescott, S.; Ballard, M.J.; Rizzardo, E.; Bilbert R.G. *Macromolecules* 2002, 35(14), 5417-25.
42. Wang, J.; Matyjaszewski, K. *J Am Chem Soc* 1995, 117, 5614-5615.
43. Matyjaszewski, K.; Xia, J. *Chem. Rev.* 2001, 101(9), 2921-2990.
44. Min K.; Gao, H.; Matyjaszewski, K. *J Am Chem Soc* 2006, 128(32), 10521-10526.
45. Davis, KA; Paik, H-j.; Matyjaszewski, K. *Macromolecules*, 1999, 32(6), 1767-76.
46. Kajiwara, A.; matyjaszewski, K. *Macromolecules*, 1998, 31(17), 5695-5701.
47. Inoue, Y.; Matyjaszewski, K. *Macromolecules*, 2004, 37, 4014-4021.
48. Shipp, D. A.; Matyjaszewski, K. *Macromolecules* 1999, 32, 2948-2955.
49. Florentina, M.; Pavel, J. *Dispersion Sci Technol* 2004, 25, 1-16.
50. Matyjaszewski, K. *Chemistry--A European Journal* 1999, 5, 3095-3102.
51. Chan-seng, D; Georges, M. K. *J Polym Sci A Polym Chem* 2006, 44, 4027-4038.
52. Schork, F. J.; Luo, YW.; Smulders, W.; Russum, J.P.; Butte, A.; Fontenot, K. *Adv Polym Sci* 2005, 175, 129-255.

53. Hutchinson, R. A.; Paquet, D.A. J.; McMinn, J.H.; Beuermann, S.; Fuller, R.E.; Jackson, C. D.  
ECHEMA Monographier 1995, 131, 467-492.
54. Hutchinson, R.A.; Beuermann, S.; Paquet, D.A.Jr.; McMinn, J.H. Macromolecules 1997, 30,  
3490-3493.
55. Beuermann, S.; Paquet, D.A.Jr.; McMinn, J.H.; Hutchinson, R.A. Macromoleculer 1996, 29,  
4206

## Appendix

### Two examples of experimental reproducibility

Experiments were conducted to evaluate reproducibility for BA on AGET ATRP microemulsion.

Exp.1 and 2 is one example and Exp. 3 and 4 is another one. The plots of conversion vs. time indicate good reproducibility. Experimental conditions list as following,

Exp.1: [BA] : [EBiB] : [CuBr<sub>2</sub>] : [BPMODA] : [ascorbic acid] = 265 : 1 : 0.49 : 0.78 : 0.19,  
[CTAB]/[BA] = 36.2 wt %

Exp.2: [BA] : [EBiB] : [CuBr<sub>2</sub>] : [BPMODA] : [ascorbic acid] = 329 : 1 : 0.56 : 0.82 : 0.22,  
[CTAB]/[BA] = 36.8 wt %

Exp.3 [BA] : [EBiB] : [CuBr<sub>2</sub>] : [BPMODA] : [ascorbic acid] = 379 : 1 : 1.3 : 1.9 : 0.44,  
[CTAB]/[BA] = 27.5 wt%

Exp.4 [BA] : [EBiB] : [CuBr<sub>2</sub>] : [BPMODA] : [ascorbic acid] = 387 : 1 : 1.3 : 1.9 : 0.42,  
[CTAB]/[BA] = 27.8 wt%

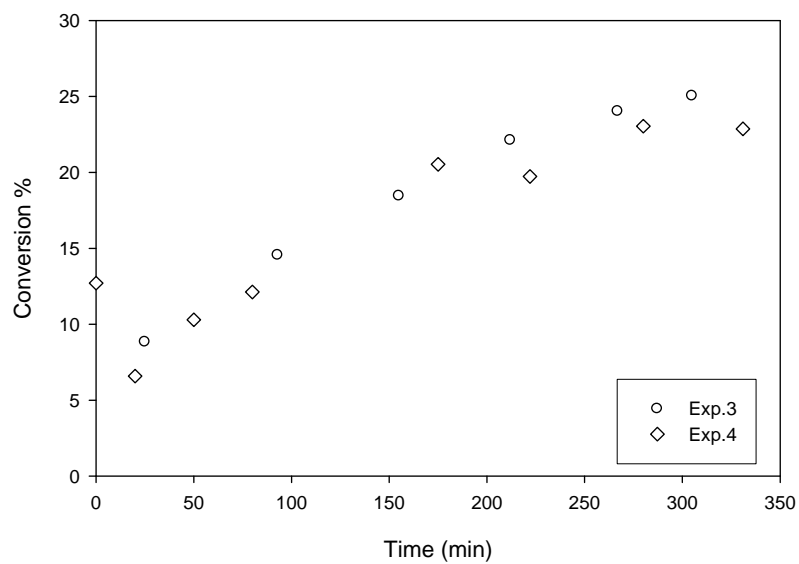
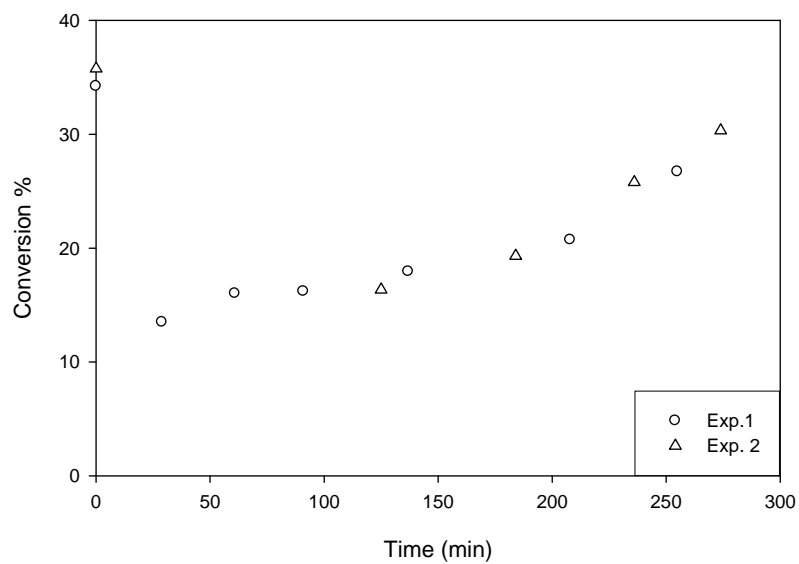


**Figure A- 1 Evolution of conversion in reproducibility of BA in AGET ATRP microemulsion.**

**Reaction Tem = 80°C.**

### **NMR spectrum**

The following NMR spectrum was for the synthesis ligand BPMODA.

The chemical shift of all NMR peaks agreed with the literature<sup>(51)</sup>; <sup>1</sup>H NMR (CDCl<sub>3</sub>, δ, ppm), 8.5 (d, 2H), 7.65 (t, 2H), 7.55 (d, 2H), 3.8 (s, 4H), 2.55 (t, 2H), 1.6-1.2 (m, 32), 0.9 (t, 3H).

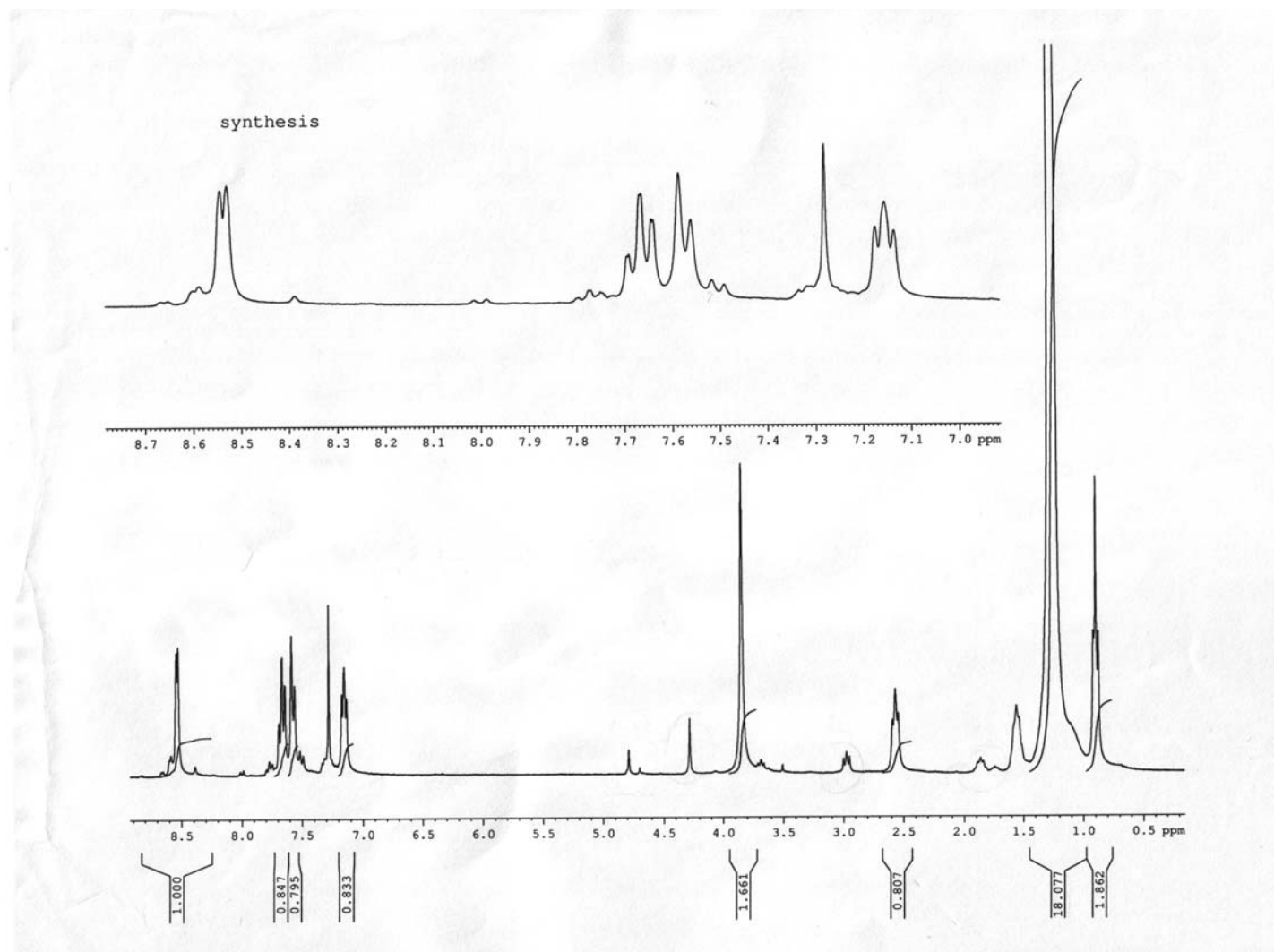


Figure A- 2  $^1\text{H}$  NMR spectra of ligand BPMODA